

Large N Optimization for Multi-Matrix Systems

Robert de Mello Koch,^{a,b} Antal Jevicki,^c Xianlong Liu,^c Kagiso Mathaba^b and João P. Rodrigues^b

^a*School of Science, Huzhou University,
Huzhou 313000, China*

^b*National Institute for Theoretical and Computational Sciences,
School of Physics and Mandelstam Institute for Theoretical Physics,
University of the Witwatersrand, Wits, 2050, South Africa*

^c*Department of Physics, Brown University,
182 Hope Street, Providence, RI 02912, USA*

E-mail: robert@neo.phys.wits.ac.za, antal_jevicki@brown.edu,
xianlong_liu@brown.edu, 0601228x@students.wits.ac.za,
Joao.Rodrigues@wits.ac.za

ABSTRACT: In this work we revisit the problem of solving multi-matrix systems through numerical large N methods. The framework is a collective, loop space representation which provides a constrained optimization problem, addressed through master-field minimization. This scheme applies both to multi-matrix integrals ($c = 0$ systems) and multi-matrix quantum mechanics ($c = 1$ systems). The complete fluctuation spectrum is also computable in the above scheme, and is of immediate physical relevance in the later case. The complexity (and the growth of degrees of freedom) at large N have stymied earlier attempts and in the present work we present significant improvements in this regard. The (constrained) minimization and spectrum calculations are easily achieved with close to 10^4 variables, giving solution to Migdal-Makeenko, and collective field equations. Considering the large number of dynamical (loop) variables and the extreme nonlinearity of the problem, high precision is obtained when confronted with solvable cases. Through numerical results presented, we prove that our scheme solves, by numerical loop space methods, the general two matrix model problem.

Contents

1	Introduction	1
2	Overview	3
2.1	Collective (Loop Space) Representation	5
2.2	Loop Space Inequalities and Constrained Minimization	7
2.3	Master Field	9
3	Methods	11
3.1	Loop truncation	11
3.2	Optimization Procedure	14
4	SD Models	16
4.1	Single Matrix Systems	16
4.2	Two-Matrix Systems	17
4.3	Results	17
5	Matrix Quantum Mechanics Spectrum	21
5.1	Fluctuations	21
5.2	One-Matrix Example	23
5.3	Two-Matrix example	24
6	Conclusions	32
A	Analytic Results for Matrix Integrals	33
A.1	Quartic Model	33
A.2	Quadratic Two-Matrix Model	34
A.3	Cubic Model	34
B	Analytical Results of The One-Matrix Quantum Mechanics	35

1 Introduction

Large N multi-matrix problems are at the center of many theories of current interest, involving membranes [1], reduced super Yang-Mills theories [2–6], field theory of critical and noncritical strings [7–22], phase transitions and black holes [23–31], and M-matrix theory [32]. At the same time, apart from very special cases, these systems are not solvable due to the fact that they are highly nonlinear. At finite N one has numerical Monte-Carlo methods [33], which have provided definite and most relevant results [32] with increase of simulations towards large N . The limiting theory, infinite N , features a rapid growth of

the degrees of freedom, represented by (Wilson) loop variables, which are physical, gauge invariant collective variables for the description of matrix and non-Abelian gauge theories. As is well known, (Wilson) loops become independent degrees of freedom at infinite N , and the exact theory is governed by non-linear Schwinger-Dyson (Migdal-Makeenko) equations [34], or alternatively in the collective field theory representation, in terms of an effective action [35] and/or a collective Hamiltonian [36]. The latter provides a unified approach in which $1/N = G$ appears as a coupling constant, and has been used through the years for non perturbative studies. For coupled systems (of matrices) at quantum level, only simple systems are solvable. However, numerical approaches were developed in [37, 38]. In these previous studies the nature of the (infinite N) planar solution was understood as related to a constrained minimization problem, where a significant role is played by a set of inequalities associated with invariants (loops) in the collective description. An effective scheme for dealing with this constrained minimization was identified, through the use of master-field variables [38]. These methods were also seen to apply at sub-leading order in N and in particular, to consideration of the spectrum [39, 40].

Recently, there is a renewed interest in large N optimization [41], with studies [42–44] that overlap with earlier work, and which re-discover the importance of loop space inequality constraints.

Due to potential high relevance in problems of emergent geometry, thermalization and black hole formation we revisit the earlier collective field constrained minimization and numerical master field methods, with interest in increasing the numbers of degrees of freedom, and the potential for high precision results. These are developed in the present work. For concreteness, and with purpose of making comparisons (with analytical results, when possible) we mostly deal with systems of two hermitian matrices, but the methods are seen to apply for any number, with arbitrary single or multi trace interactions.

The content of this paper is as follows: In the overview Section 2 we provide a short summary of the collective large N method [38]. In particular, the infinite N constrained minimization scheme is summarized, featuring the associated complete set of (loop space) inequalities. We then give a summary of the unconstrained master variable method which applies for the large N ground state and also for spectrum studies [39, 40]. We explain the study of multi-matrix integrals through the Hamiltonian description [45] given by Fokker-Planck. In Section 3 we describe the numerical methods used for constrained minimization. In Section 4 we give a list of models studied and present the numerical solution of the associated matrix integrals. In Section 5 we present results, giving numerical solutions for one- and two-matrix large N quantum Hamiltonian problems. At the large N level these essentially correspond to giving a (numerical) solution of the fully nonlinear Schwinger-Dyson equations with approximately 10^4 loop variables. Correspondingly methods (and evaluation) of large N ground state energies, gaps and low lying spectra are also given. Conclusions and future applications to problems of interest are commented in Section 6.

2 Overview

In this article we will study and develop numerical techniques for solving the large N multi-matrix theories. We will consider two classes of the multi-matrix systems. The first one is the multi-matrix integral ($c = 0$ systems) whose partition function reads

$$\int \prod_{l=1}^d dM_l e^{-S(M_1, M_2, \dots, M_d)}, \quad (2.1)$$

where $S(M)$ is a multi trace action. The second one is matrix quantum mechanics (MQM) ($c = 1$ systems), whose dynamics is given by a Hamiltonian of the form

$$H = \frac{1}{2} \text{Tr}(\Pi_1^2 + \Pi_2^2 + \dots + \Pi_d^2) + V(M_1, M_2, \dots, M_d), \quad (2.2)$$

where Π_l is the canonical conjugate of M_l .

The large N expansion in the *collective field formulation* is developed after a change of variables from the original matrix valued variables to invariant variables, which we refer to as “loops”. This terminology has its origins in lattice gauge theory, where the basic field degrees of freedom are unitary matrices U_l , one for each link in the lattice. In that case the invariant variables, Wilson loops $\phi(C)$, are obtained by taking the trace of an ordered product of unitary matrices, one for each link of a closed path C . It is common to continue to refer to invariant variables as “loops” even for theories of hermitian matrices M_l where invariants are given by the trace of products of the matrices. As an example, for the case of two hermitian matrices we have

$$\phi(C) = \text{Tr}(M_1^{n_1} M_2^{n_2} M_1^{n'_1} M_2^{n'_2} \dots). \quad (2.3)$$

In this case the invariant $\phi(C)$ is not labeled by a closed path, but rather by specifying a word C in the alphabet of the matrices. The word specifies the order in which matrices are multiplied before tracing. The invariant loop variables are then described by all of the words with cycling identification. For example, $\text{Tr}(M_1 M_1 M_2)$ is equal to $\text{Tr}(M_1 M_2 M_1)$ and $\text{Tr}(M_2 M_1 M_1)$ due to the cyclicity of trace, hence they all refer to the same invariant loop variable. It is in this sense that we use the loop terminology. For the purpose of counting the number of loops, it is useful to enumerate the loops with a permutation σ . The loop corresponding to permutation σ is denoted ϕ_σ . Consider loops built as single trace products of n M_1 s and m M_2 s. The permutation $\sigma \in S_{n+m}$ specifies the loop ϕ_σ as follows

$$\begin{aligned} \phi_\sigma &= \text{Tr}(\sigma M_1^{\otimes n} M_2^{\otimes m}) \\ &= (M_1)_{i_1 i_{\sigma(1)}} \cdots (M_1)_{i_n i_{\sigma(n)}} (M_2)_{i_{n+1} i_{\sigma(n+1)}} \cdots (M_2)_{i_{n+m} i_{\sigma(n+m)}}. \end{aligned} \quad (2.4)$$

The cycle structure of the permutation translates into the trace structure of ϕ_σ . For a single trace σ must be an $n+m$ cycle. This parametrization is not unique as distinct permutations do not necessarily define distinct loops. This follows by noting that

$$\begin{aligned} \phi_{\tau^{-1}\sigma\tau} &= \text{Tr}(\sigma\tau M_1^{\otimes n} M_2^{\otimes m} \tau^{-1}) \\ &= (M_1)_{i_{\tau(1)} i_{\sigma(\tau(1))}} \cdots (M_1)_{i_{\tau(n)} i_{\sigma(\tau(n))}} (M_2)_{i_{\tau(n+1)} i_{\sigma(\tau(n+1))}} \cdots (M_2)_{i_{\tau(n+m)} i_{\sigma(\tau(n+m))}}, \end{aligned} \quad (2.5)$$

so that if $\tau \in S_n \times S_m =$ the permutation group swapping M_1 s with each other and M_2 s with each other, then

$$\phi_{\tau^{-1}\sigma\tau} = \phi_\sigma. \quad (2.6)$$

In general, two loops ϕ_{σ_1} and ϕ_{σ_2} are the same if

$$\tau^{-1}\sigma_1\tau = \sigma_2 \quad (2.7)$$

for some $\tau \in S_n \times S_m$. Removing this redundancy, we are left with a complete set of (infinitely many) loops. To develop some intuition for this description, note that if τ belongs to the cyclic group \mathbb{Z}_{n+m} generated by the $n+m$ cycle given by $(123 \cdots n+m)$, then the equality (2.6) expresses nothing but the cyclicity of the trace. In general, we need to divide by more than just cyclicity and (2.6) is a convenient way to correctly account for all redundancies.

A relevant class of observables for the $c=0$ systems are provided by correlation functions of the loops

$$\begin{aligned} \langle \phi(C) \rangle &= \left\langle \text{Tr} (M_1^k M_2^l M_3^m \cdots) \right\rangle \\ &= \int \prod_{a,b=1}^N \prod_{l=1}^d d(M_l)_{ab} e^{-S} \text{Tr} (M_1^k M_2^l M_3^m \cdots). \end{aligned} \quad (2.8)$$

These expectation values can be determined through equations of motion for the loop expectation values. The loop equation is derived as a Schwinger-Dyson equation for the loops. In the case of a theory of unitary matrices the equation of motion for the Wilson loops are known as the Migdal-Makeenko loop equations [34]. For the case of hermitian matrices, the loop equations follow by inserting the matrix derivative under the integral:

$$0 = \int \prod_{l=1}^d dM_l \sum_{a=1}^d \frac{\partial}{\partial(M_a)_{ij}} \left(\frac{\partial \phi(C)}{\partial(M_a)_{ji}} e^{-S} \right). \quad (2.9)$$

The loop equation is a quadratic equation in the large N limit which takes the form

$$\sum_{C_1, C_2} p(C; C_1, C_2) \langle \phi(C_1) \rangle \langle \phi(C_2) \rangle - \sum_s j(C, s; C') \left\langle \phi(C') \frac{\partial S}{\partial \phi(s)} \right\rangle = 0. \quad (2.10)$$

The integer $p(C; C_1, C_2)$ specifies the number of ways in which a loop C can be split into loops C_1 and C_2 , while the integer $j(C, s; C')$ specifies the number of ways loops C and s can be joined to produce C' . Both will be described in detail below. Solving these non-linear coupled equations is highly non-trivial. Using collective field theory one obtains an effective potential which, when minimized, gives the large N solution to the Schwinger-Dyson equations.

As for the $c=1$ MQM systems, changing to invariant variables we obtain a collective potential V_{col} , which when minimized, again determines the large N expectation values of loops. These will be discussed in detail below.

2.1 Collective (Loop Space) Representation

The collective representation of multi-matrix systems can be given both at the action level for matrix integrals ($c = 0$), and at the Hamiltonian level for coupled quantum mechanical ($c = 1$) systems. These are closely related, so in formulating numerical methods one can work in the Hamiltonian framework [36]. To proceed, let us define the adjoint of the loop variable. For a loop $\phi(C)$, we define its adjoint as $\phi(\bar{C})$, where \bar{C} is the reverse of the word C . For example, for a word $C = abaab$, where $a = M_1$ and $b = M_2$, its reverse is $\bar{C} = baaba$. In hermitian matrix models, this corresponds to taking a hermitian conjugate of the matrix products. As such the adjoint $\phi(\bar{C})$ is simply the complex conjugate of $\phi(C)$ in hermitian matrix systems:

$$\phi(\bar{C}) = \bar{\phi}(C). \quad (2.11)$$

The “bar” symbol on the right hand side of the above formula denotes complex conjugate. We note in the hermitian one-matrix models case, the adjoint of a loop is itself since all loops are real valued. The use of the loop adjoints makes the hermiticity of the collective representation manifest as we will see below.

Matrix integrals. Let us start with the collective representation of the multi-matrix integral problem with any number d of matrices which at large N is efficiently described using an effective action. This is obtained by a change of integration variables (from matrices to loops)

$$\int \prod_{a,b=1}^N \prod_{l=1}^d d(M_l)_{ab} e^{-S} = \int \prod_C d\phi(C) J(\phi) e^{-S} = \int \prod_C d\phi(C) e^{-S_{\text{eff}}}, \quad (2.12)$$

resulting in a large N collective action $S_{\text{eff}} = S - \ln J$. The main ingredient in this effective description is the Jacobian J and its form is in general specified by the collective formalism. Variation of this collective action correctly produces the Schwinger-Dyson (SD) equations (2.9). The derivative of the collective action [35] gives

$$\bar{\omega}(C) - \sum_{C'} \Omega(C, C') \frac{\partial S}{\partial \phi(C')} = 0. \quad (2.13)$$

The functional $\omega(C)$ stands for

$$\omega(C; \phi) \equiv 2\hat{E}_l^\alpha \hat{E}_l^\alpha \phi(C) = \sum_{(C_1, C_2)} p(C; C_1, C_2) \phi(C_1) \phi(C_2), \quad (2.14)$$

representing the splitting of contour C into sub-contours (C_1, C_2) .¹ The split occurs at the pinched link, so in general there are several distinct ways for the process, which necessitates the sum. The integer $p(C; C_1, C_2)$ counts the number of ways loop C can be partitioned, by the splitting operation, into loops C_1 and C_2 . In a similar way one has

$$\Omega(C_1, C_2; \phi) \equiv -2\hat{E}_l^\alpha \bar{\phi}(C_1) \hat{E}_l^\alpha \phi(C_2) = \sum_C j(C_1, C_2; C) \phi(C) \quad (2.15)$$

¹For unitary $(M_l)_{ab}$ matrices, $\hat{E}_l^\alpha = \sqrt{2} t_{ab}^\alpha (M_l)_{bc} \frac{\partial}{\partial (M_l)_{ac}}$. The generators of the Lie algebra of $U(N)$ are normalized such that $\sum_\alpha t_{ab}^\alpha t_{a'b'}^\alpha = \frac{1}{2} \delta_{ab'} \delta_{a'b}$. For hermitian matrix systems, $\hat{E}_l^\alpha \rightarrow \hat{E}_l^{ab} = -i \frac{\partial}{\partial (M_l)_{ba}}$, with $(M_l)_{ab}$ hermitian.

for the opposite operation of joining contours. We note the use of loop adjoint in the definition. The integer $j(C_1, C_2; C)$ counts the number of ways in which C_1 and C_2 can be joined to produce C . A computer algorithm was developed to generate loops and also these loop processes which we call *loop algebra*.

For numerical minimization it is useful to follow [45], where it was established (through a stochastic quantization) that the above SD problem can be represented through (Fokker-Planck type) the quantum mechanical Hamiltonian: $H = K + V_{\text{eff}}$. The solution of nonlinear SD equations is then obtained by minimization of an effective potential of the following form

$$V_{\text{eff}} = \frac{1}{8} \bar{\omega}(C) \Omega^{-1}(C, C') \omega(C') - \frac{1}{4} \bar{\omega}(C) \frac{\partial V}{\partial \phi(C)} + \frac{1}{8} \overline{\frac{\partial S}{\partial \phi(C)}} \Omega(C, C') \frac{\partial S}{\partial \phi(C')}, \quad (2.16)$$

where the “bar” symbols again denote complex conjugates. This effective potential also gives the leading large N configuration of the bosonic sector of multi matrix Marinari-Parisi [46] type models. Expansion around the stationary point leads to equations for small fluctuations and a systematic $1/N$ expansion scheme.

Matrix quantum mechanics. We now describe the collective field formulation of the large N MQM in detail. Considering a general multi-matrix quantum mechanics problem, in the operator formalism, one has a transition to the collective description by performing a change to curvilinear (loop space) variables (with a Jacobian J) which induces the collective Hamiltonian, taking the form

$$H_{\text{col}} = \frac{1}{2} \sum_{C, C'} \pi^\dagger(C) \Omega(C, C') \pi(C') + V_{\text{col}}[\phi] \quad (2.17)$$

with

$$V_{\text{col}}[\phi] = \frac{\hbar}{8} \sum_{C, C'} \bar{\omega}(C) \Omega^{-1}(C, C') \omega(C') + V[\phi], \quad (2.18)$$

and $\pi(C)$ representing the conjugates to the loops $\phi(C)$. Here $V[\phi]$ is the original potential written in terms of loops. The collective Hamiltonian is manifestly hermitian, and is equivalent to the original MQM Hamiltonian (2.2). We have used the notation V_{col} to denote the *collective potential* obtained for MQM systems, which plays an analogue role of the effective potential V_{eff} for matrix integral problems, as described above.

Notation emphasis. To proceed, let us emphasize that throughout we will use V_{eff} to denote the *effective potential* associated with matrix integrals ($c = 0$ systems), and V_{col} to denote the *collective potential* associated with MQM ($c = 1$ systems).

Large N background and fluctuation spectrum. In the next subsection we explain that the $N \rightarrow \infty$ limit is obtained by minimizing the potential V_{eff} or V_{col} and that this minimization is subject to a sequence of inequalities which constrain the range of the loop variables. The relevance of constrained minimization becomes even more fundamental when one proceeds to study the spectrum at large N . Ordinarily this would be given directly in

loop space by expanding about the stationary field

$$\phi(C) = \phi_0(C) + \frac{1}{N}\eta(C), \quad (2.19)$$

$$\pi(C) = NP(C), \quad (2.20)$$

and reducing the collective Hamiltonian to a quadratic, small fluctuation Hamiltonian

$$H_{\text{col}}^{(2)} = \frac{N^2}{2} \sum_{C,C'} P^\dagger(C) \Omega^0(C, C') P(C') + \frac{1}{2N^2} \sum_{C,C'} \bar{\eta}(C) V^{(2)}(C, C') \eta(C'), \quad (2.21)$$

$$\Omega^0(C, C') = \Omega(C, C') \Big|_{\phi_0(C)}, \quad V^{(2)}(C, C') = \frac{\partial^2 V_{\text{col}}}{\partial \bar{\phi}(C) \partial \phi(C')} \Big|_{\phi_0(C)}. \quad (2.22)$$

This $H^{(2)}$, and its diagonalization provides the spectrum at large N . Essentially, it is determined by eigenvalues of the matrix:

$$\varepsilon_i^2 = \text{eig}(\Omega^0 V^{(2)}) = \text{eig}(V^{(2)} \Omega^0). \quad (2.23)$$

As we will explain next, these are to be found subject to obeying a set of (loop) space inequalities that are central for reaching the correct minima.

2.2 Loop Space Inequalities and Constrained Minimization

Positivity of the loop joining matrix Ω . In the collective Hamiltonian description, the $N \rightarrow \infty$ limit (and the sum of planar diagrams) is given by the semiclassical approximation. The problem is therefore to solve for the static stationary configuration denoted $\phi_0(C)$, which minimizes the potential V_{col} . This would be generally given by the equation

$$\frac{\partial V_{\text{col}}[\phi]}{\partial \phi(C)} = 0. \quad (2.24)$$

However, as was understood earlier [37, 38], in the minimization a role is also played by a sequence of inequalities (analogous to Schwarz inequalities) which constrain the range of loop variables. Such a sequence of inequalities is generic, and will be present for any set of variables representing invariants. In the collective description the inequalities are directly visible and can be generally specified and given in terms of the loop space matrix Ω . This matrix participates in the kinetic term of the Hamiltonian and defines the loop space symplectic form. As such the matrix Ω must be positive semi-definite. Indeed from the definition of the matrix Ω one has the fact that it can be written as

$$\Omega(C, C') = \sum_i \bar{A}_{iC} A_{iC'} = \sum_i A_{Ci}^\dagger A_{iC'}, \quad (2.25)$$

i.e. it is explicitly *positive semi-definite*. Indeed, in our case, defining²

$$A_{iC} \equiv \frac{\partial \phi(C)}{\partial (M_l)_{ab}}, \quad i \equiv (a, b, l), \quad (2.26)$$

²Here we consider the case that $(M_l)_{ab}$ is a unitary matrix, but the same conclusion holds when $(M_l)_{ab}$ is hermitian.

we obtain

$$\begin{aligned}
\Omega(C, C') &= -2 \sum_{\alpha} \hat{E}^{\alpha} \bar{\phi}(C) \hat{E}^{\alpha} \phi(C') \\
&= 2 \sum_{l\alpha} (M_l^{\dagger})_{ca} t_{ab}^{\alpha} \frac{\partial \bar{\phi}(C)}{\partial (M_l^{\dagger})_{cb}} t_{a'b'}^{\alpha} (M_l)_{b'c'} \frac{\partial \phi(C')}{\partial (M_l)_{a'c'}} \\
&= \sum_l \frac{\partial \bar{\phi}(C)}{\partial (M_l^{\dagger})_{cb}} \frac{\partial \phi(C')}{\partial (M_l)_{bc}} = \sum_l \frac{\partial \bar{\phi}(C)}{\partial (\bar{M}_l)_{bc}} \frac{\partial \phi(C')}{\partial (M_l)_{bc}} \\
&= \sum_i \bar{A}_{iC} A_{iC'} .
\end{aligned}$$

Positivity constraints. *The minimization therefore must be done subject to the positivity condition of the loop joining matrix Ω . In general the positive semi-definiteness of the loop valued matrix Ω gives the complete set of inequalities, which schematically reads*

$$\text{eig}(\Omega(C, C')) \geq 0. \quad (2.27)$$

We can write the complete set of these generalized loop space (Schwarz) inequalities as follows. A convenient basis (and explicit form) turns out to be given by the sequence of the sub-determinants $\det_k(\Omega) \geq 0$. The sub-determinant is defined by (repeated indices are summed)

$$\begin{aligned}
\det_l(\Omega) &= \frac{1}{l!(N_{\Omega} - l)!} \epsilon_{C_1 \dots C_l a_1 \dots a_{N_{\Omega} - l}} \epsilon_{C_1 \dots C_l a_1 \dots a_{N_{\Omega} - l}} \Omega(C_1, C'_1) \dots \Omega(C_l, C'_l) \\
&= \frac{1}{l!(N_{\Omega} - l)!} \epsilon_{C_1 \dots C_l a_1 \dots a_{N_{\Omega} - l}} \epsilon_{C'_1 \dots C'_l a_1 \dots a_{N_{\Omega} - l}} \bar{A}_{i_1 C_1} A_{i_1 C'_1} \dots \bar{A}_{i_l C_l} A_{i_l C'_l} \\
&= \bar{T}_{i_1 \dots i_l a_1 \dots a_{N_{\Omega} - l}} T_{i_1 \dots i_l a_1 \dots a_{N_{\Omega} - l}}, \quad (2.28)
\end{aligned}$$

where N_{Ω} is the dimension of the loop space joining matrix Ω and

$$T_{i_1 \dots i_l a_1 \dots a_{N_{\Omega} - l}} = \frac{1}{\sqrt{l!(N_{\Omega} - l)!}} \epsilon_{C'_1 \dots C'_l a_1 \dots a_{N_{\Omega} - l}} A_{i_1 C'_1} \dots A_{i_l C'_l}. \quad (2.29)$$

The expression in the last line of (2.28) makes the positivity of the sub-determinant manifest. An alternative formula for the sub-determinant is provided by

$$\det_l(\Omega) = \chi_{(1^l)}(\Omega), \quad (2.30)$$

where $\chi_{(1^l)}(\cdot)$ is a Schur polynomial and (1^l) is the Young diagram with a single column and l rows. This formula is simple with the normalization chosen in (2.28). The sub-determinant basis is particularly useful when some of the constraints are saturated, in which case certain eigenvalues of Ω vanish. If p eigenvalues vanish, then there are p independent vanishing sub-determinants

$$\det_k(\Omega) = 0, \quad k = N_{\Omega} - p + 1, N_{\Omega} - p + 2, \dots, N_{\Omega}. \quad (2.31)$$

Once expressed in terms of loops, this positivity condition implies highly non-trivial inequality constraints among the $\phi(C)$'s. The positivity inequalities constrain the eigenvalues of the loop space matrix Ω , leading to a constrained minimization of V_{eff} or V_{col} .³ The stationary minimum solution is generally characterized by saturation of a certain number of inequalities, whereby the loop space matrix Ω develops zero eigenvalues.

2.3 Master Field

A most complete way to deal with the constrained optimization at large N is through variables that *automatically* assure the positivity condition of the loop space matrix Ω . These are the *master field variables*, or simply the original matrix valued variables of the system. In terms of such variables the expectation values of loops are determined by a direct stationary-point equation of the loop space effective ($c = 0$) or collective ($c = 1$) potential

$$\frac{\partial}{\partial(M_l)_{ab}} V_{\text{eff/col}} = 0. \quad (2.32)$$

Here the notation $V_{\text{eff/col}}$ represents either V_{eff} or V_{col} . This saddle-point equation in terms of the master variables is correct in all phases of the theory, both the weak- and strong-coupling. Let us also mention how the correct loop-space equation follows from the master equation. Multiplying and summing over the appropriate factors, we obtain

$$\sum_{ab,l} \sum_{C'} \frac{\partial \bar{\phi}(C)}{\partial(\bar{M}_l)_{ab}} \frac{\partial \phi(C')}{\partial(M_l)_{ab}} \frac{\partial V_{\text{eff/col}}}{\partial \phi(C')} = \sum_{C'} \Omega(C, C') \frac{\partial V_{\text{eff/col}}}{\partial \phi(C')} = 0, \quad (2.33)$$

This fact that the saddle-point equation in terms of the master variable produces the correct loop-space equation can be taken as another argument for the existence of the master field.

Denote the set of master variables and their complex conjugates by ϕ_α and $\bar{\phi}_\alpha$, respectively. To see that the positivity of Ω is assured when working in terms of the master variables, note that we can write Ω as

$$\Omega(C, C') = \sum_{\alpha} \frac{\partial \bar{\phi}(C)}{\partial \bar{\phi}_\alpha} \frac{\partial \phi(C')}{\partial \phi_\alpha} = \sum_{\alpha} A_{C\alpha}^\dagger A_{\alpha C'}, \quad A_{\alpha C} = \frac{\partial \phi(C)}{\partial \phi_\alpha}. \quad (2.34)$$

The set $\{\phi_\alpha, \bar{\phi}_\alpha\}$ is always assumed to be at least as large as the set of invariants $\{\phi(C)\}$. We can think of these variables as the original variables of the theory, in which case they transform non-trivially under the existing internal symmetries and form a larger set than that of the invariants that can be obtained from them. Nevertheless, we have also other situations in mind: one may truncate the effective potential, in which case the number of ϕ_α variables must be larger than the number of loop variables included in the potential. In general, the set $\{\phi_\alpha\}$ is at least as large as the set of invariants. This is the case in one-matrix models, for instance, where one identifies the ϕ_α 's with the matrix eigenvalues.

³Numerically and for unitary matrices systems, one finds that down to a certain critical value of the coupling, a standard unconstrained minimization procedure converges giving the correct minima. However, at a critical point (and below) the procedure breaks down. For single unitary matrix systems this is the Gross-Witten phase transition [47], also present in the single unitary matrix hamiltonian systems [48–50].

The important characteristic of these variables then is that they solve the positivity constraint explicitly. Therefore, in the large- N limit, the ground state configuration is determined by the saddle-point condition

$$\frac{\partial V_{\text{eff/col}}}{\partial \phi_\alpha} = \sum_C \frac{\partial \phi(C)}{\partial \phi_\alpha} \frac{\partial V_{\text{eff/col}}}{\partial \phi(C)} = 0. \quad (2.35)$$

It is clear that it is useful to reduce the problem to unconstrained minimization. In [37, 38] we have presented and tested numerically such a framework developing a hybrid loop space + master field approach. The use of master variables [38] is simple. In terms of the original variables the inequalities are *automatically* obeyed so we can think of changing back to these master variables but keeping the collective loop space Hamiltonian. This is because it is the loop space Hamiltonian that generates the $1/N$ expansion. Now the ground state and the fluctuation spectrum will be given by unconstrained minimization, satisfying

$$\frac{\partial V_{\text{eff/col}}[\phi(C\{\phi_\alpha\})]}{\partial \phi_\alpha} = 0, \quad \forall \phi_\alpha. \quad (2.36)$$

This represents an implicit equation for the master field ϕ_α since it enters $V_{\text{eff/col}}$ through the loop variables $\phi(C\{\phi_\alpha\})$. As such it is not very useful at the analytic level but it can be easily implemented numerically [37].

We will consider systems of two hermitian matrices in this article. Systems of hermitian matrices are always in the phase in which some of the constraints are saturated. Consequently for these systems the use of master variables is of particular importance. The loop invariants consist of single trace products of these matrices. As a result, one of the matrices can be chosen to be diagonal, and the other will be parametrized in the Lie algebra of the unitary group. The master variables are then real, which is something we use in the following.⁴

The master eigenvalue equations for the fluctuation spectrum are similarly obtained in this hybrid scheme. Denote in our Hamiltonian formulation the master field solution by ϕ_α^0 . We are then led to appropriate spectrum eigenvalue equations through a shift in the loop space collective Hamiltonian. One essentially considers a ‘canonical’ transformation [40] from loops to master fields

$$P_\beta = \sum_C \frac{\partial \phi(C)}{\partial \phi_\beta} \Big|_{\phi_\alpha^0} P(C), \quad \eta_\beta = \sum_C \left[\frac{\partial \phi(C)}{\partial \phi_\beta} \Big|_{\phi_\alpha^0} \right]^{-1} \eta(C), \quad (2.37)$$

to obtain the following quadratic Hamiltonian

$$H^{(2)} = \frac{1}{2} \sum_\alpha P_\alpha P_\alpha + \frac{1}{2} \sum_{\alpha, \beta} \eta_\alpha \mathcal{M}_{\alpha\beta} \eta_\beta. \quad (2.38)$$

Note that the term linear in η vanishes as a result of equation (2.35). The mass matrix $\mathcal{M}_{\alpha\beta}$ is then to be computed from

$$\mathcal{M}_{\alpha\beta} = \frac{\partial \bar{\phi}(C)}{\partial \phi_\alpha} \Big|_{\phi_\alpha^0} \frac{\partial^2 V_{\text{col}}}{\partial \bar{\phi}(C) \partial \phi(C')} \Big|_{\phi_0\{\phi_\alpha^0\}} \frac{\partial \phi(C')}{\partial \phi_\beta} \Big|_{\phi_\alpha^0}. \quad (2.39)$$

⁴The general case is discussed in [40].

Here the repeated indices C and C' are summed, which in principle range from 1 to infinity. To compute it numerically we must perform the truncation discussed below. The fluctuation spectrum is obtained by solving for the square root of the nonzero eigenvalues of the mass matrix. In Section 5 we will show in detail that this is equivalent to the direct computation of fluctuation spectrum in loop space.

We will see that in numerical evaluations of multi-matrix problems, the hybrid loop space + master field formalism turns out to be advantageous, converging rapidly and giving excellent agreement already at small loop and color cutoffs. With interest in precision optimization we will furthermore test the method for larger sizes and number of minimization variables ($\sim 9 \times 10^3$).

3 Methods

3.1 Loop truncation

A numerical implementation of the large N minimization of the collective potential necessarily involves a truncation of the infinite dimensional loop space. We will truncate the loop space by restricting to loops that limit the number of matrices appearing in the trace to be smaller than some fixed cut off L_{\max} . This loop truncation is reminiscent of level truncation in string field theory [51]. To gather some insight into this truncation, in this section we consider the counting of loops as a function of the cut off. A convenient approach towards this counting uses permutations to enumerate loops.

Loop counting. Consider the hermitian two-matrix model. The truncation of loop space that we employ restricts $n+m \leq L_{\max}$ a fixed maximum loop length, where n and m denote the number of M_1 and M_2 in a loop, respectively. It is interesting to count the number of loops as a function of L_{\max} . This counting is a useful input to the numerical implementation since it specifies how many variables appear in the numerical minimization. There is an extremely rapid growth of the number of loops with increasing L_{\max} . The counting problem can be solved with a standard application of Polya theory [52]. We start by introducing the single letter partition function, which for two matrices is

$$Z_1 = x + y. \tag{3.1}$$

The single trace partition function, which counts the number of loops, is now given by

$$\begin{aligned} F(x, y) &= \sum_n \sum_{n|d} \frac{\varphi(d)}{n} Z_1(x^d, y^d)^{\frac{n}{d}} \\ &= \sum_{n,m=1}^{\infty} \mathcal{N}_{n,m} x^n y^m. \end{aligned} \tag{3.2}$$

The sum is over all integers n . At each n there is a second sum over d which runs over the divisors of n , i.e. all the integers that can be divided into n without remainder. The function $\varphi(d)$ is the Euler totient function. The degree L contribution to $F(x, y)$ counts single trace operators constructed from L matrices. The coefficient $\mathcal{N}_{n,m}$ of the monomial

of degree n in x and degree m in y counts the number of loops that can be constructed using n M_1 s and m M_2 s. The first few terms of $F(x, y)$ are

$$\begin{aligned}
F(x, y) = & (x + y) + (x^2 + xy + y^2) + (x^3 + x^2y + xy^2 + y^3) \\
& + (x^4 + x^3y + 2x^2y^2 + xy^3 + y^4) \\
& + (x^5 + x^4y + 2x^3y^2 + 2x^2y^3 + xy^4 + y^5) \\
& + (x^6 + x^5y + 3x^4y^2 + 4x^3y^3 + 3x^2y^4 + xy^5 + y^6) + \dots
\end{aligned} \tag{3.3}$$

To interpret this answer, note that for example, the contribution $2x^3y^2$ implies that there are two independent loops that can be constructed using $3M_1$ s and $2M_2$ s. These two loops are $\text{Tr}(M_1^3M_2^2)$ and $\text{Tr}(M_1^2M_2M_1M_2)$.

To explore how the total number of loops grows, it is useful to consider the blind partition function, obtained by setting $y = \alpha = x$. The coefficient of α^n counts the total number of loops constructed using n matrices. The blind partition function is

$$\begin{aligned}
F(\alpha, \alpha) = & 2\alpha + 3\alpha^2 + 4\alpha^3 + 6\alpha^4 + 8\alpha^5 + 14\alpha^6 + 20\alpha^7 + 36\alpha^8 + 60\alpha^9 + 108\alpha^{10} + 188\alpha^{11} \\
& + 352\alpha^{12} + 632\alpha^{13} + 1182\alpha^{14} + 2192\alpha^{15} + 4116\alpha^{16} + 7712\alpha^{17} + 14602\alpha^{18} \\
& + 27596\alpha^{19} + 52488\alpha^{20} + 99880\alpha^{21} + 190746\alpha^{22} + 364724\alpha^{23} + 699252\alpha^{24} \\
& + 1342184\alpha^{25} + 2581428\alpha^{26} + 4971068\alpha^{27} + 9587580\alpha^{28} + \dots
\end{aligned} \tag{3.4}$$

demonstrating an extremely rapid growth in the number of invariants (loops).

Loop space truncation. Our numerical implementation of loop space dynamics truncates to the subspace of invariants, given by all loops with $L_{\max} = 2l - 2$ matrices or less in the trace. In this scheme Ω is an $N_\Omega \times N_\Omega$ matrix, where N_Ω is the number of loops with l matrices or less in the trace. Ω itself depends on a total of N_{Loops} , which is the number of loops with $2l - 2$ matrices or less. For this reason, our minimization scheme minimizes with respect to N_{Loops} independent variables. The values of L_{\max} , N_Ω and N_{Loops} for values $3 \leq l \leq 10$ are given in Table 1 below.

L_{\max}	N_Ω	N_{Loops}
4	9	15
6	15	37
8	23	93
10	37	261
12	57	801
14	93	2615
16	153	8923
18	261	31237

Table 1: Truncating loop space.

For the minimization, we parametrize M_1 and M_2 using $N + N^2$ real valued master variables. These are the N eigenvalues for M_1 and the N^2 matrix elements in M_2 . For a given l we must choose the number of colors N large enough that $N^2 + N \geq N_{\text{Loops}}$. To obtain the large N background, our numerical experiments focus on $l = 9$, so that we keep a total of 8923 loops. We choose $N = 94$ so that there are a total of 8930 master variables.

Spectrum calculation. To obtain the fluctuation spectrum based on master variables, one needs to preserve the matrix structure of the loop derivatives (3.7) with respect to both M_1 and M_2 . We then truncate the mass matrix equation (2.39) as follows

$$\mathcal{M}_{ij} = \sum_{C, C'=1}^{N_{\text{Loops}}} \bar{A}_{iC} \Big|_{\phi_\alpha^0} \frac{\partial^2 V_{\text{col}}}{\partial \bar{\phi}(C) \partial \phi(C')} \Big|_{\phi_0 \{ \phi_\alpha^0 \}} A_{jC'} \Big|_{\phi_\alpha^0}, \quad i, j = 1, \dots, 2N^2. \quad (3.5)$$

Here the “bar” symbols represent the complex conjugate. The mass matrix $\mathcal{M}_{\alpha\beta}$ is a matrix of dimension

$$2N^2 \times 2N^2,$$

obtained from the multiplication of

$$[2N^2 \times N_{\text{Loops}}] \times [N_{\text{Loops}} \times N_{\text{Loops}}] \times [N_{\text{Loops}} \times 2N^2]$$

matrices. It is essential that one sums over all N_{Loops} in the equation above.⁵ One obtains N_Ω nonzero eigenvalues and $2N^2 - N_\Omega$ (numerically) zero eigenvalues.

We now observe that

$$\widehat{\Omega}^0(C, C') \equiv \sum_i \bar{A}_{iC} \Big|_{\phi_\alpha^0} A_{iC'} \Big|_{\phi_\alpha^0}, \quad C, C' = 1, \dots, N_{\text{Loops}},$$

is a $(N_{\text{Loops}} \times N_{\text{Loops}})$ matrix which, in loop space, would include all loops up to length $4l - 6$. In practice, it is not feasible to obtain such $\widehat{\Omega}$ directly in loop space, given the size of the truncations considered in this article (e.g., for $l = 9$, $4l - 6 = 30$). However, it can be generated from the master variables.

The nonzero eigenvalues of (3.5) can then be matched with those of the loop space spectrum matrix

$$\mathcal{M}_{C, C''} = \sum_{C'=1}^{N_{\text{Loops}}} \widehat{\Omega}_0(C, C') V^{(2)}(C', C''), \quad C, C'' = 1, \dots, N_{\text{Loops}}. \quad (3.6)$$

This is a $N_{\text{Loops}} \times N_{\text{Loops}}$ matrix, and is expressed explicitly in terms of loop variables. It has N_Ω nonzero eigenvalues and $N_{\text{Loops}} - N_\Omega$ (numerically) zero eigenvalues. Throughout, we have checked that the nonzero eigenvalues of (3.5) and (3.6) are identical.

⁵Indeed, it was shown in [40] that if the sum is restricted to N_Ω loops, every non-zero eigenvalue of (2.23) is also an eigenvalue of (3.5), with N_{Loops} replaced by N_Ω . Except in the strong coupling phase of unitary matrix systems, the spectrum obtained simply on the basis of (2.23), with Ω^0 a $(N_\Omega \times N_\Omega)$ matrix is not accurate.

3.2 Optimization Procedure

A Python code was developed to obtain the computational results. The first step is to generate all the distinct single trace loops of a given length l . There are different ways of generating them, including using `Mathematica` and Polya theory. A simple procedure is to generate the list of C_l^n combinations for $0 \leq n \leq l$, which index the position of (say) the matrix M_2 in the string (word) of M_1 and M_2 matrices, and then remove loops which are identical up to cyclic permutations. They are then indexed and stored as a list of arrays, eg. $[1, 1, 1], [1, 1, 2], [1, 2, 2], [2, 2, 2]$, etc., and stacked for different lengths, to obtain the list of N_Ω and N_{Loops} loops described in Section 3.1, reproducing Table 1. The zeroth indexed element of the list is the empty array corresponding to $\phi(0) = \text{Tr}(\mathbf{I})/N = 1$. It is fixed throughout.

The next step is to generate the loop joining matrix Ω

$$\Omega(c, c') = \sum_{a=1}^2 \frac{\partial \bar{\phi}(c)}{\partial (M_a)_{ij}} \frac{\partial \phi(c')}{\partial (M_a)_{ji}} = \sum_{c''=0}^{N_{\text{Loops}}} j(c, c'; c'') \phi(c''), \quad c, c' = 1, \dots, N_\Omega.$$

Here we use little ‘ c ’ instead of capital ‘ C ’ to emphasize the loop truncation: the loop joining matrix Ω now is a finite matrix of dimension $N_\Omega \times N_\Omega$ instead of an infinite dimensional matrix. The code implements explicitly the first equality in the above equation, recalling that⁶

$$\begin{aligned} \frac{\partial}{\partial (M_1)_{ij}} \text{Tr}(\dots M_1 \dots) &= \frac{\partial}{\partial (M_1)_{ij}} \text{Tr}(M_1 g(\dots M_1 \dots M_2 \dots)) + \dots \\ &= g_{ji}(\dots M_1 \dots M_2 \dots) + \dots \end{aligned} \quad (3.7)$$

(g_{ij} is obtained by extracting M_1 from the loop). The joined loop $\phi(c'')$ is identified, and the *nonzero* joining coefficients $j(c, c'; c'')$ are stored. It should be emphasized that, through a joining process higher loops are generated, and the $N_\Omega \times N_\Omega$ matrix Ω contains higher loops up to length N_{Loops} . It is this full set of loops contained in and generated by Ω that will participate in the optimization process.

A similar procedure is followed to generate ω defined through loop splitting

$$\omega(c) = \sum_{a=1}^2 \frac{\partial}{\partial (M_a)_{ij}} \frac{\partial \phi(c)}{\partial (M_a)_{ji}} = \sum_{c', c''=0}^{N_{\text{Loops}}} p(c; c', c'') \phi(c') \phi(c''), \quad c = 1, \dots, N_\Omega.$$

The split loops $\phi(c'), \phi(c'')$ are identified, and the *nonzero* splitting coefficients $p(c; c', c'')$ are stored. Since a given loop always splits into two smaller loops, ω only depends on the subset of N_Ω loop variables.

The master variables are the $N \times N$ matrices M_1 and M_2 . For the minimization, due to the single trace nature of the invariant loops, M_1 is chosen diagonal and M_2 is an arbitrary $N \times N$ hermitian matrix which we parametrize in the Lie algebra of $U(N)$

$$(M_1)_{ij} = \sum_{a=1}^N \mathbf{a}_{aa} t_{ij}^{aa}, \quad (M_2)_{ij} = \sum_{a=1}^N \mathbf{b}_{aa} t_{ij}^{aa} + \sum_{a < b}^N \mathbf{b}_{ab} t_{ij}^{ab} + \sum_{a > b}^N \mathbf{b}_{ab} t_{ij}^{ab}.$$

⁶in the equation below ‘ \dots ’ stands for terms generated when the derivative does not act on the M_1 shown on the left hand side of the first line.

Here t_{ij}^{ab} ($a < b$) is the set of real off-diagonal generators (σ_1 in the entries (ij) and (ji)). t_{ij}^{ab} ($a > b$) are the purely imaginary generators (σ_2 in the entries (ij) and (ji)), and t_{ij}^{aa} are the entries of a diagonal matrix.

In order to extract the explicit dependence on the powers of N from the loops, they are defined as

$$\phi(c) = \text{Tr}(\cdots M_1 \cdots M_2 \cdots M_1 \cdots M_2 \cdots) / N^{\frac{\text{len}(c)}{2}+1}, \quad (3.8)$$

where $\text{len}(c)$ is length of the word c , i.e. the number of matrices in the loop.

The function to be minimized is (2.16) for matrix integrals or (2.18) for matrix quantum mechanics. The argument of the function is the real concatenated array $\mathbf{a}_{aa}, a = 1, \dots, N$ with the flattened matrix array $\mathbf{b}_{ab}, a, b = 1, \dots, N$. At each iteration, for a given configuration of master variables, the N_{Loops} loops are evaluated from (3.8) and Ω and ω are evaluated with the values of the loops together with the coefficients $j(c, c'; c'')$ and $p(c; c', c'')$. Inversion of Ω is avoided by solving the relevant linear equations.

We used a standard `minimize` function from the `scipy.optimize` library. We used two methods, the `BFGS` and the `CG` methods. We found that the `BFGS` method is slightly faster, but for large loop truncations, the `CG` method is more stable. Both these methods require the evaluation of the gradient. This is achieved by calculating for each iteration the derivatives of the loops with respect to the master variables

$$\frac{\partial \phi(c)}{\partial \phi_\alpha}, \quad \phi_\alpha \equiv (\mathbf{a}_{aa}, \mathbf{b}_{ab}), \quad a, b = 1, \dots, N.$$

The initial master variables configuration consists of a randomly generated real vector and of a randomly generated real matrix. For Fokker-Planck (and the underlying $c = 0$) type systems, we have set as convergence criteria that the norm of the gradient vector becomes less than $\sqrt{N(N+1)} 10^{-16}$. In other words, at convergence, a typical gradient vector element has norm of order 10^{-16} . Convergence of the algorithm is remarkably stable, with the energy monotonically decreasing to zero in successive iterations. Depending on the size of the truncation, the energy at convergence is $\sim 10^{-24} - 10^{-31}$. The norm of the gradient components typically range from $\sim 10^{-15} - 10^{-20}$. At convergence, the Schwinger-Dyson equations are satisfied to typical accuracy $\sim 10^{-10} - 10^{-18}$. With a 3.0 GHz Mac, the codes take from about a few seconds for $N_{\text{Loops}} = 37$, about two hours for $N_{\text{Loops}} = 2615$ and more than a day for $N_{\text{Loops}} = 8923$.

For spectra of the MQM ($c = 1$) systems discussed in 5, we use $N = 94$ to generate large N background. The initial master variables configuration again consists of a randomly generated real vector and of a randomly generated real matrix. The convergence criteria is that the norm of the gradient vector becomes less than $\sqrt{N(N+1)} 10^{-16}$. Again, for $N_{\text{Loops}} = 37$, converge is achieved in hours, while for $N_{\text{Loops}} = 8923$ convergence takes days.

For a given loop truncation size N_{Loops} , starting with the lowest N satisfying $N(N+1) \geq N_{\text{Loops}}$ and increasing N , loop values are seen not to change much. Loop values quickly converge to their exact values (when known) as N_{Loops} is increased. This is particularly so for the N_Ω small loops. This is evidenced, for example, in the matrix integrals case, in Table 8.

4 SD Models

As a first application of the methods outlined above, we will study matrix integrals. For these models (in the decoupled case) there are exact analytic calculations which can be used to validate our numerical results. In all cases we are able to confirm that our numerical results are essentially exact for loops of lower length, with the accuracy falling off as we approach L_{\max} which is the maximal length of loops admitted in the minimization. We note that all these models have a Hamiltonian quantum mechanical interpretation (Fokker-Planck). We also consider a variety of problems with two matrices to demonstrate the methods. It will be clear that the extensions to more matrices proceed in the same way, without difficulty.

Numerically we are evaluating the integral (2.8) with the action S given by

$$S = V(M_1) + V(M_2) + k \operatorname{Tr}(M_1 M_2), \quad (4.1)$$

where the potential is given by

$$V(M) = \frac{1}{2} \operatorname{Tr}(M^2) + \frac{g_3}{\sqrt{N}} \operatorname{Tr} M^3 + \frac{g_4}{N} \operatorname{Tr} M^4. \quad (4.2)$$

When the coupling $k = 0$ we will refer to the system as a “single matrix system” and when $k \neq 0$ as a “two-matrix system”. Note however, that for both types of systems we evaluate mixed loops $\phi(C)$ obtained by tracing products involving both matrices M_1 and M_2 , so that even when $k = 0$ the problem is still a multi matrix problem.

4.1 Single Matrix Systems

Free theory. The potential of the zero dimensional model is

$$V(M) = \frac{1}{2} \operatorname{Tr} M^2, \quad (4.3)$$

so that we have set $g_3 = g_4 = 0$. We also set $k = 0$. The effective potential is

$$V_{\text{eff}} = \frac{1}{8} \omega \Omega^{-1} \omega + \frac{1}{8} \operatorname{Tr}(M_1^2) + \frac{1}{8} \operatorname{Tr}(M_2^2) - \frac{1}{2} N^2. \quad (4.4)$$

Quartic theory. The potential of the corresponding zero dimensional model is

$$V(M) = \frac{1}{2} \operatorname{Tr} M^2 + \frac{g_4}{N} \operatorname{Tr} M^4, \quad (4.5)$$

so that we have set $k = g_3 = 0$. The effective potential is

$$\begin{aligned} V_{\text{eff}} = & \frac{1}{8} \omega \Omega^{-1} \omega + \left(\frac{1}{8} - 2g_4 \right) \operatorname{Tr}(M_1^2) + \left(\frac{1}{8} - 2g_4 \right) \operatorname{Tr}(M_2^2) - \frac{1}{2} N^2 \\ & - \frac{g_4}{N} (\operatorname{Tr}(M_1)^2 + \operatorname{Tr}(M_2)^2) + \frac{g_4}{N} (\operatorname{Tr}(M_1^4) + \operatorname{Tr}(M_2^4)) \\ & + \frac{2g_4^2}{N^2} (\operatorname{Tr}(M_1^6) + \operatorname{Tr}(M_2^6)). \end{aligned} \quad (4.6)$$

Cubic model. We use

$$V(M) = \frac{1}{2}\text{Tr}M^2 + \frac{g_3}{\sqrt{N}}\text{Tr}M^3, \quad (4.7)$$

so that we have set $k = g_4 = 0$. The effective potential is

$$\begin{aligned} V_{\text{eff}} = & \frac{1}{8}\omega\Omega^{-1}\omega + \frac{1}{8}\text{Tr}(M_1^2) + \frac{1}{8}\text{Tr}(M_2^2) + \frac{3g_3}{4\sqrt{N}}\text{Tr}(M_1^3) + \frac{3g_3}{4\sqrt{N}}\text{Tr}(M_2^3) - \frac{1}{2}N^2 \\ & + \frac{9g_3^2}{8N}\text{Tr}(M_1^4) + \frac{9g_3^2}{8N}\text{Tr}(M_2^4) - \frac{3g_3}{2\sqrt{N}}\text{Tr}(M_1) - \frac{3g_3}{2\sqrt{N}}\text{Tr}(M_2). \end{aligned} \quad (4.8)$$

4.2 Two-Matrix Systems

Quadratic model. The potential of the zero dimensional model is

$$V(M) = \frac{1}{2}\text{Tr}M^2, \quad (4.9)$$

so that we have set $g_3 = g_4 = 0$. In this case we keep $k \neq 0$. The effective potential is

$$V_{\text{eff}} = \frac{1}{8}\omega\Omega^{-1}\omega + \frac{k^2+1}{8}\text{Tr}(M_1^2) + \frac{k^2+1}{8}\text{Tr}(M_2^2) + \frac{k}{4}\text{Tr}(M_1M_2) - \frac{1}{2}N^2. \quad (4.10)$$

Coupled cubic two-matrix model. We keep $k > 0$ and we set

$$V(M) = \frac{1}{2}\text{Tr}M^2 + \frac{g_3}{\sqrt{N}}\text{Tr}M^3, \quad (4.11)$$

so that we have set $g_4 = 0$. The effective potential is

$$\begin{aligned} V_{\text{eff}} = & \frac{1}{8}\omega\Omega^{-1}\omega + \frac{1+k^2}{8}\text{Tr}(M_1^2) + \frac{1+k^2}{8}\text{Tr}(M_2^2) + \frac{k}{4}\text{Tr}(M_1M_2) - \frac{1}{2}N^2 \\ & + \frac{3g_3}{4\sqrt{N}}\text{Tr}(M_1^3) + \frac{3g_3}{4\sqrt{N}}\text{Tr}(M_2^3) + \frac{9g_3^2}{8N}\text{Tr}(M_1^4) + \frac{9g_3^2}{8N}\text{Tr}(M_2^4) \\ & + \frac{3g_3k}{4\sqrt{N}}\text{Tr}(M_1^2M_2) + \frac{3g_3k}{4\sqrt{N}}\text{Tr}(M_1M_2^2) - \frac{3g_3}{2\sqrt{N}}\text{Tr}(M_1) - \frac{3g_3}{2\sqrt{N}}\text{Tr}(M_2). \end{aligned} \quad (4.12)$$

4.3 Results

In tables 2-10 we present results for SD models, obtained with $l = 9$ and $N = 94$.⁷ The results show that for small loops we essentially obtain the exact answer. For larger loops (with more than l matrices in the trace, in the notation of Section 3) the results are less accurate, but even for the longest loops accuracy is typically always better than 5%.

⁷In the following tables the traces are scaled by appropriate factors according to (3.8) so that the results of loops are independent of the matrix size N .

g_4	0		1		10	
	Exact	Numerical	Exact	Numerical	Exact	Numerical
$\text{Tr}(M_1^2)$	1	0.9999565	0.3125	0.3139285	0.113752	0.1166236
$\text{Tr}(M_1 M_2)$	0	0.0002630	0	8.846×10^{-6}	0	0.0002037
$\text{Tr}(M_1^4)$	2	1.9998894	0.171875	0.1732885	0.0221562	0.0230570
$\text{Tr}(M_1^2 M_2^2)$	1	0.9999058	0.0976563	0.09810712	0.0129395	0.0132793
$\text{Tr}(M_1^6)$	5	4.9997429	0.113281	0.11462865	0.00513368	0.0054013
$\text{Tr}(M_1^2 M_2^4)$	2	1.9998074	0.0537109	0.05394868	0.00252031	0.0025842
$\text{Tr}(M_1^4 M_2^2)$	2	1.9997449	0.0537109	0.05415388	0.00252031	0.0026246
$\text{Tr}(M_1^4 M_2^4)$	4	3.9994546	0.029541	0.02977492	0.000490897	0.0005107

Table 2: Results for the $g_3 = k = 0$ as g_4 is varied. The table shows loops with lengths ≤ 8 .

g_4	0		1		10	
	Exact	Numerical	Exact	Numerical	Exact	Numerical
$\text{Tr}(M_1^{10})$	42	41.898479	0.0629883	0.064156	0.000350126	0.000376
$\text{Tr}(M_1^8 M_2^2)$	14	13.986907	0.0256348	0.026020	0.000148213	0.000157
$\text{Tr}(M_1^5 M_2^5)$	0	0.014260	0.0	1.030×10^{-5}	0.0	-5.322×10^{-7}
$\text{Tr}(M_1^{12})$	132	130.63810	0.050354	0.051447	0.0000978653	0.000106
$\text{Tr}(M_1^6 M_2^6)$	25	25.130274	0.0128326	0.012996	2.635×10^{-5}	2.779×10^{-5}
$\text{Tr}(M_1^{14})$	429	417.95735	0.041458	0.042414	2.816×10^{-5}	3.053×10^{-5}
$\text{Tr}(M_1^4 M_2^{10})$	84	84.278562	0.0108261	0.010975	7.757×10^{-6}	8.111×10^{-6}
$\text{Tr}(M_1^{16})$	1430	1359.7222	0.0349121	0.035647	8.283×10^{-6}	8.941×10^{-6}

Table 3: Results for the $g_3 = k = 0$ as g_4 is varied. The loops shown have lengths ≥ 10 and ≤ 16 .

g_3	0.01		0.025		0.05	
	Exact	Numerical	Exact	Numerical	Exact	Numerical
$\text{Tr}(M_1^2)$	1.00363	1.00363	1.02358	1.02358	1.11155	1.11155
$\text{Tr}(M_1 M_2)$	0.000906539	0.000909	0.00589	0.00589	0.027799	0.027798
$\text{Tr}(M_1^4)$	2.02182	2.02182	2.14427	2.14429	2.73465	2.73462
$\text{Tr}(M_1^2 M_2^2)$	1.00727	1.00727	1.04771	1.04771	1.23554	1.23554
$\text{Tr}(M_1^6)$	5.10951	5.10950	5.73859	5.73869	9.1135	9.1131
$\text{Tr}(M_1^2 M_2^4)$	2.02915	2.02916	2.19482	2.19485	3.0397	3.03967
$\text{Tr}(M_1^4 M_2^2)$	2.02915	2.02915	2.19482	2.19485	3.0397	3.03967
$\text{Tr}(M_1^4 M_2^4)$	4.08777	4.08779	4.59788	4.59810	7.47831	7.47913

Table 4: Results for $g_4 = k = 0$ as g_3 is varied. The table shows loops with lengths ≤ 8 .

g_3	0.01		0.025		0.05	
	Exact	Numerical	Exact	Numerical	Exact	Numerical
$\text{Tr}(M_1^{10})$	44.3207	44.2172	58.4568	58.3197	156.937	156.449
$\text{Tr}(M_1^8 M_2^2)$	14.5658	14.5441	17.9569	17.9432	39.9365	39.8981
$\text{Tr}(M_1^5 M_2^5)$	0.207449	0.2311	1.4793	1.5072	10.4007	10.4477
$\text{Tr}(M_1^{12})$	142.267	140.851	207.031	204.9967	732.18	723.9593
$\text{Tr}(M_1^6 M_2^6)$	26.1071	26.2563	32.9314	33.1235	83.0558	83.4798
$\text{Tr}(M_1^{14})$	473.759	462.0533	767.231	748.6339	3570.97	3476.2509
$\text{Tr}(M_1^4 M_2^{10})$	89.6086	89.8709	125.347	125.4809	429.168	427.3324
$\text{Tr}(M_1^{16})$	1623.11	1546.8709	2943.81	2808.6594	17971.5	17086.8

Table 5: Results for $g_4 = k = 0$ as g_3 is varied. The loops shown have lengths ≥ 10 and ≤ 16 .

k	0		$\frac{1}{2}$		$\frac{3}{4}$	
	Exact	Numerical	Exact	Numerical	Exact	Numerical
$\text{Tr}(M_1^2)$	1	0.9999565	1.33333	1.333362	2.28571	2.28559
$\text{Tr}(M_1 M_2)$	0	0.0002630	-0.666667	-0.666619	-1.71429	-1.71416
$\text{Tr}(M_1^4)$	2	1.999885	3.55556	3.555304	10.449	10.447
$\text{Tr}(M_1^2 M_2^2)$	1	0.9999058	2.22222	2.221766	8.16327	8.16228
$\text{Tr}(M_1^6)$	5	4.9997429	11.8519	11.8497	59.7085	59.6988
$\text{Tr}(M_1^2 M_2^4)$	2	1.9998074	6.51852	6.51612	44.035	44.0271
$\text{Tr}(M_1^4 M_2^2)$	2	1.9997449	6.51852	6.51603	44.035	44.0271
$\text{Tr}(M_1^4 M_2^4)$	4	3.9994546	19.9506	19.9388	256.0	255.9

Table 6: Results for $g_3 = g_4 = 0$ as k is varied. The table shows loops with length ≤ 8 .

k	0		$\frac{1}{2}$		$\frac{3}{4}$	
	Exact	Numerical	Exact	Numerical	Exact	Numerical
$\text{Tr}(M_1^{10})$	42	41.898479	176.988	178.1885	2620.35	2649.95
$\text{Tr}(M_1^8 M_2^2)$	14	13.986907	88.4938	88.7473	1856.08	1869.81
$\text{Tr}(M_1^5 M_2^5)$	0	0.014260	-61.2346	-61.2468	-1605.73	-1610.73
$\text{Tr}(M_1^{12})$	132	130.63810	741.663	759.5443	18823.7	19572.3
$\text{Tr}(M_1^6 M_2^6)$	25	25.130274	263.111	264.3137	11215.9	11339.8
$\text{Tr}(M_1^{14})$	429	417.95735	3213.87	3378.6847	139833	151758
$\text{Tr}(M_1^4 M_2^{10})$	84	84.278562	1170.09	1169.2822	84618.9	85304.5
$\text{Tr}(M_1^{16})$	1430	1359.7222	14283.9	15516.1101	1.0654×10^6	1.2204×10^6

Table 7: Results for $g_3 = g_4 = 0$ as k is varied. The loops shown have lengths ≥ 10 and ≤ 16 .

N_{Loops}	93	93	261	261	801	801
N_{Ω}	23	23	37	37	57	57
N	10	12	16	18	28	30
$\text{Tr}(M_1^2)$	1.398558	1.398550	1.398602	1.398606	1.398608	1.398608
$\text{Tr}(M_1 M_2)$	0.724017	0.724014	0.724058	0.724062	0.724064	0.724064
$\text{Tr}(M_1^4)$	4.078131	4.075882	4.083250	4.083690	4.083917	4.083920
$\text{Tr}(M_1^2 M_2^2)$	2.584743	2.584708	2.588234	2.588669	2.588752	2.588754
$\text{Tr}(M_1^6)$	14.627466	13.991341	15.388399	15.430672	15.477357	15.477725
$\text{Tr}(M_1^2 M_2^4)$	8.479602	8.622227	8.692989	8.740663	8.739481	8.739705
$\text{Tr}(M_1^4 M_2^2)$	8.404034	8.284243	8.688555	8.727894	8.738072	8.738460
$\text{Tr}(M_1^4 M_2^4)$	56.718119	52.025168	63.460122	64.980069	66.088900	66.155167

Table 8: Results for $g_3 = 0.05$, $k = 0.5$ for $l = 5, 6, 7$ and increasing N . Note that the length of the last loop is > 7 .

N_{Loops}	37	93	261	801	2615	8923
N_{Ω}	15	23	37	57	93	153
ε_1	0.49236511	0.49236370	0.49236470	0.49236443	0.49236443	0.49236463
ε_2	0.49342716	0.49343864	0.49344212	0.49344752	0.49344586	0.49344757

Table 9: The two lowest lying states for $k = g_4 = 0$ and $g_3 = 0.05/3 = 0.0167$.

N_{Loops}	37	93	261	801	2615	8923
N_{Ω}	15	23	37	57	93	153
ε_1	5.44592002	5.25941037	5.13024606	5.20001164	5.18903527	5.15228747
ε_2	5.81626188	5.33316170	5.41489587	5.40011675	5.36702168	5.33021481

Table 10: The two lowest lying states for $k = g_3 = 0$ and $g_4 = 10$.

5 Matrix Quantum Mechanics Spectrum

In this section, we consider multi-matrix quantum mechanical models, which includes the evaluation of (Wilson) loop expectation values at large N , ground state energies at large N , and the spectrum of fluctuations (which corresponds to N^0 , i.e. order 1). The coupled two-matrix Hamiltonian reads

$$H = \frac{1}{2} \text{Tr}(\Pi_1^2 + \Pi_2^2) + V(M_1, M_2), \quad (5.1)$$

with a potential

$$V(M_1, M_2) = \frac{1}{2} \text{Tr}(M_1^2 + M_2^2) + k \text{Tr}(M_1 M_2) + \frac{g_4}{N} \text{Tr}(M_1^4 + M_2^4). \quad (5.2)$$

We note, that the SD models featured in the previous section are also of this form, but an effective potential containing double trace couplings. Consequently the numerical methods for evaluating the stationary points and the spectrum apply to both with no difference in degree of difficulty. Likewise, our methods can be applied to multi-matrix models with arbitrary number of matrices. We describe evaluation of the spectrum for the above case. For normalization purposes, we will also give numerical (and analytical) one-matrix results.

5.1 Fluctuations

The general strategy for the spectrum calculation of small fluctuations in loop space, which holds for all multi-matrix quantum mechanics in the limit of large N , has been described in previous sections, and is easily implementable on a computer. In this subsection we explain the subtlety about truncation further. As in the optimization procedure, we truncate the infinite dimensional loop space. Let l denote the chosen loop length truncation, and N_Ω denote the number of loops whose lengths are less or equal to l . Ω then is a N_Ω by N_Ω matrix which involves N_{Loops} loops in total, and the loop of maximal length it contains is $L = 2l - 2$. Sending $\Omega \rightarrow N^{-2}\Omega$, we obtain the collective Hamiltonian

$$H_{\text{col}} = \frac{1}{2N^2} \sum_{c=1}^{N_\Omega} P^\dagger(c) \Omega(c, c') P(c') + N^2 V_{\text{col}}[\phi], \quad (5.3)$$

where

$$V_{\text{col}}[\phi] = \frac{1}{8} \sum_{c=1}^{N_\Omega} \bar{\omega}(c) \Omega^{-1}(c, c') \omega(c') + v[\phi]. \quad (5.4)$$

Here $N^2 v[\phi]$ is the original potential written in terms of loops. We then expand H_{col} to order $\mathcal{O}(1)$, which is accomplished by shifting loop variables around the ground state

$$\phi(C) = \phi_0(C) + \frac{1}{N} \eta(C), \quad P(C) = N p(C), \quad \text{where } C = 1, \dots, N_{\text{Loops}}, \quad (5.5)$$

and omitting the constant background terms. We use Capital C to emphasize that here the loop labels run from 1 to N_{Loops} , instead of N_Ω , because V_{col} in equation (5.4) involves N_{Loops} independent loops. Accordingly there are also N_{Loops} canonical conjugates, which

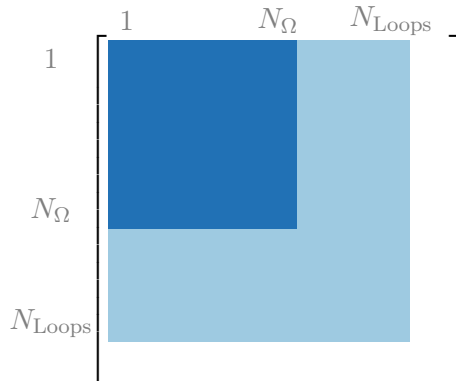


Figure 1: Illustration of Ω truncation for spectrum calculation.

requires us to use the N_{Loops} by N_{Loops} dimensional loop joining matrix denoted as $\widehat{\Omega}$. The choice of the loop joining matrix is illustrated in Figure 1, where the deep blue blocks are used for truncation in V_{col} , and the deep plus light blue blocks, i.e. $\widehat{\Omega}$, are used in the following $H_{\text{col}}^{(2)}$.

The Taylor expansion then gives

$$H_{\text{col}}^{(2)} = \sum_{C=1}^{N_{\text{Loops}}} \left(\frac{1}{2} p^\dagger(C) \widehat{\Omega}_0(C, C') p(C') + \frac{1}{2} \bar{\eta}(C) V_0^{(2)}(C, C') \eta(C') \right), \quad (5.6)$$

in which $V_0^{(2)}$ is the Hessian matrix of V_{col} at the ground state. We note that all elements in Ω are linear functions of loops. Their second derivatives therefore are 0, and hence do not contribute to $V_0^{(2)}$. For the same reason, the second derivative of $v[\phi]$ vanishes if it only contains single trace terms.

To evaluate the spectrum, one can diagonalize the kinetic term in (5.6) and then solve the eigenvalues of the resulting mass matrix. As pointed out earlier, we see that using $\widehat{\Omega}$ also resolves the mismatch of the dimensions between Ω_0 and $V_0^{(2)}$. Since $\widehat{\Omega}_0$ is positive definite, one can perform a canonical transformation

$$\eta \rightarrow \sqrt{\widehat{\Omega}_0} \eta, \quad p \rightarrow \sqrt{\widehat{\Omega}_0^{-1}} p. \quad (5.7)$$

The spectrum is then given, in terms of the *nonzero* eigenvalues of the spectrum matrix $\widehat{\Omega}_0 V_0^{(2)}$, by

$$\varepsilon_n = \left[\text{eig}_n \left(\sum_{C'=1}^{N_{\text{Loops}}} \widehat{\Omega}_0(C, C') V_0^{(2)}(C', C'') \right) \right]^{1/2}, \quad n \in \mathbb{Z}^+, \quad (5.8)$$

where eig_n denotes the n th nonzero eigenvalue. Here n starts from 1 instead of 0, because the zero mode is excluded in the definition of Ω (or $\widehat{\Omega}$). The spectrum is independent of truncation loop length l , as we will see in the following concrete examples. In principle, the size of the spectrum one can obtain is equal to the N_Ω . Besides, there are precisely $N_{\text{Loops}} - N_\Omega$ zero eigenvalues of $\widehat{\Omega}_0 V_0^{(2)}$, therefore the truncation scheme automatically

projects out the higher modes. As l is increased, higher modes are included, and one is able to obtain higher frequencies.

Depending on the size of the truncation and particularly for multi-matrix systems, it is not feasible in general to obtain $\widehat{\Omega}_0$ directly in loop space. But $\widehat{\Omega}_0$ can be always be constructed with master variables. The spectrum equation (5.8) then takes the form

$$\varepsilon_n = \left[\text{eig}_n \left(\sum_{C'=1}^{N_{\text{Loops}}} \sum_a \sum_{i,j} \frac{\partial \bar{\phi}(C)}{\partial (\bar{M}_a)_{ij}} \frac{\partial \phi(C')}{\partial (M_a)_{ji}} V_0^{(2)}(C', C'') \right) \right]^{1/2}. \quad (5.9)$$

For example, the spectrum that is presented in Section 5.3 is obtained in the background of 801 (this is the number of loops for a cut off of $L_{\text{max}} = 2 \times 7 - 2$) loops, whose value is determined by the master field after minimization. This results in a spectrum eigenvalue matrix of size $\approx 10^3 \times 10^3$. Note also that 401 947 loops are effectively included in the computation of $\widehat{\Omega}_0$. This is only possible through the use of master variables and a direct loop space evaluation would not be possible. It is visible that the spectrum calculation in terms of master fields should give the same results, except for different numbers of zero eigenvalues of $\widehat{\Omega}_0 V_0^{(2)}$.

We observe that in the free theory cases, interestingly, one can actually obtain exact results by working with a smaller $V_0^{(2)}$ matrix, whose matrix indices range only from 1 to N_Ω , and correspondingly with the smaller Ω_0 matrix. This has been verified in both one- and two-matrix quantum mechanics. This is no longer the case the moment coupling constants are switched on.

5.2 One-Matrix Example

We then proceed to employ our general strategy to compute the spectrum of the hermitian one-matrix quantum mechanics:

$$H = -\frac{1}{2} \text{Tr} \left(\frac{\partial^2}{\partial M^2} \right) + \frac{1}{2} \text{Tr}(M^2) + \frac{g_4}{N} \text{Tr}(M^4). \quad (5.10)$$

In this simple case the all loop variables are real, and are labeled by a nonnegative integer n so that $\phi(n) = \text{Tr}(M^n)/N^{n/2+1}$. The loop joining and splitting have components

$$\Omega(n, m) = N^{-2} n m \phi(n + m - 2), \quad \omega(n) = n \sum_{m=0}^{n-2} \phi(m) \phi(n - m - 2). \quad (5.11)$$

Some analytical results including the spectrum formula are summarized in Appendix B. With the analytical loop values (B.4) we can also obtain the spectrum using a computer. A `Mathematica` program was developed for the spectrum calculation. The one-matrix case has the simple feature that $N_\Omega = l$ and also $N_{\text{Loops}} = L_{\text{max}}$, which provides us a canonical example to illustrate our general strategy. To calculate the spectrum using the general strategy at loop length truncation $l = 6$, for example, there are totally $L_{\text{max}} = 10$ loops contained in V_{col} . Ω_0 then is a 6×6 matrix, but $\widehat{\Omega}_0$ and $V_0^{(2)}$ are both 10×10 matrices. In Table 11 we present both the exact (B.7) and numerical low lying spectrum results for

g_4	exact results					numerical results				
	0	0.1	1	10	100	0	0.1	1	10	100
ε_1	1	1.223	2.014	4.037	8.557	1	1.223	2.014	4.037	8.557
ε_2	2	2.447	4.027	8.074	17.115	2	2.447	4.027	8.074	17.115
ε_3	3	3.67	6.041	12.111	25.672	3	3.67	6.041	12.111	25.672
ε_4	4	4.894	8.055	16.148	34.23	4	4.894	8.055	16.148	34.229
ε_5	5	6.117	10.069	20.185	42.787	5	6.117	10.069	20.189	42.798
ε_6	6	7.34	12.082	24.222	51.344	6	7.34	12.083	24.229	51.362

Table 11: One-matrix spectrum.

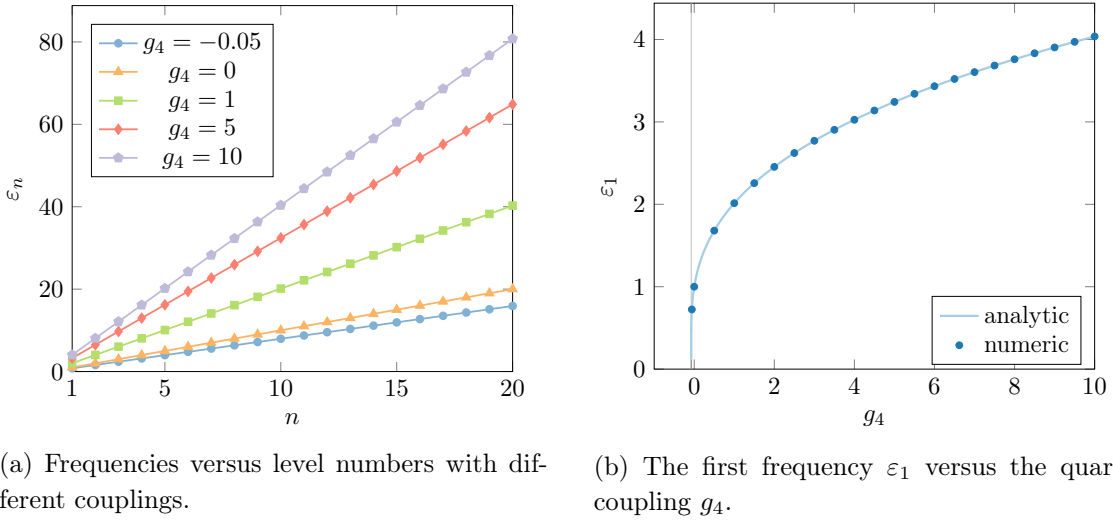


Figure 2: Spectrum of the large N Hermitian one-matrix quantum mechanics.

various g_4 , showing excellent agreement. These results are also relevant to the following two-matrix example. In Figure 2a we present several numerical results of spectrum ε_n versus level indices n . They all fit into a straight line, revealing the simple relation $\varepsilon_n = n\varepsilon_1$, which is also a property predicted by the exact result (B.7). When $g_4 = 0$, the model reduces to decoupled harmonic oscillators, therefore we have $\varepsilon_n = n$, as is verified. For other couplings we present the first level frequency ε_1 in Figure 2b. The exact and numerical results again agree very well, including the critical region $g \sim g_c = -1/3\sqrt{2}\pi$.

5.3 Two-Matrix example

By applying the same strategy, and using the numerical minimization results, we are also able to evaluate the spectrum of the hermitian two-matrix quantum mechanics (5.1) and (5.2), using a *Mathematica* program.

At first we present in Table 12 the comparison of the ground state energies, in which the two-matrix results are obtained from numerical minimization, and the one-matrix results

g_4	2×one-matrix	two-matrix
0	1	1
0.1	1.08479	1.08479
1	1.48047	1.48044
10	2.68896	2.68894
100	5.54551	5.54549

Table 12: $E_{\text{gs}}^{(0)}$ comparison.

are obtained from the analytical expression (B.5). The two-matrix model in $c = 0$ cases doubles the one-matrix model interaction, and one expects that the ground state energy should therefore be twice that of the corresponding one-matrix result. Table 12 exhibits excellent agreement, verifying the expectation.

As for the spectrum computation, the multi-matrix models lose the simple feature $N_\Omega = l$, and a rapid growth of N_Ω has already been observed in the two-matrix case. Based on the $l = 9$ ($l = 7$) numerical minimization data for interacting (free) case, we present some spectrum results evaluated at truncation $l = 4, 5, 6, 7$ in Table 13, 14, 15, 16 and 17. Taking the $l = 6$ case for example, one has $N_\Omega = 37$, so that Ω in V_{eff} is 37×37 . On the other hand, the fact $L = 10$ requires us to use the $N_{\text{Loops}} = 261$ dimensional $\widehat{\Omega}_0$ and $V_0^{(2)}$, which implies a large amount ($261 - 37 = 224$) of the zero eigenvalues of $\widehat{\Omega}_0 V_0^{(2)}$. This was verified by our `Mathematica` program. Comparing the two-matrix spectrum results, we see that as l is increased, low lying spectrum are stable and convergent, and higher level frequencies are obtained.

Let us now examine in more detail the primary characteristics of the two-matrix spectra. As the results show, in free theory, $k = g_4 = 0$, the spectrum values coincide with the one-matrix case. Besides, a high degeneracy pattern is observed. Let $\mathcal{N}(n)$ denote the number of inequivalent loops of length n . The degeneracy at level n is precisely equal to $\mathcal{N}(n)$. For instance, at level 2 the degeneracy is 3, since there are 3 independent loops, namely $\text{Tr}(M_1 M_1)$, $\text{Tr}(M_1 M_2)$, and $\text{Tr}(M_2 M_2)$. As we turn on the quartic coupling g_4 while fixing $k = 0$, the degeneracy is lifted slightly, and a different degeneracy pattern is obtained. Comparing with the one-matrix results Table 11, one can obviously see that the two-matrix spectrum contains the corresponding one-matrix spectrum as a subset, and with a degeneracy number 2. These subsets are filled in light blue colors in each $k = 0$ and $g \neq 0$ column of the two-matrix spectrum results. When turning on coupling k , the degeneracy patterns are nearly destroyed. The lifting of the degeneracy due to k and g_4 is presented in Figure 3 based on data in Table 15. We conjecture that these properties are *universal* for multi-matrix models.

k	0	0	0	0	0	0.5	0.5	0.5
g_4	0	0.1	1	10	100	0	0.1	1
ε_1	1	1.225	2.025	4.072	8.642	0.707	1.011	1.904
ε_2	1	1.225	2.026	4.079	8.644	1.225	1.422	2.148
ε_3	2	2.314	3.542	6.883	14.46	1.414	1.946	3.444
ε_4	2	2.449	4.05	8.143	17.276	1.932	2.428	4.049
ε_5	2	2.45	4.05	8.148	17.279	2.121	2.777	4.147
ε_6	3	3.546	5.635	11.164	23.604	2.45	2.939	5.354
ε_7	3	3.546	5.635	11.178	23.607	2.639	3.418	5.784
ε_8	3	3.691	6.228	12.695	27.031	2.828	3.835	6.279
ε_9	3	3.691	6.23	12.697	27.04	3.157	3.918	6.325
ε_{10}	4	4.631	7.121	13.881	29.201	3.346	4.173	7.007
ε_{11}	4	4.773	7.684	15.324	32.436	3.674	4.397	7.418
ε_{12}	4	4.774	7.691	15.335	32.469	3.864	4.623	7.609
ε_{13}	4	4.775	7.702	15.386	32.569	3.864	4.84	7.986
ε_{14}	4	4.921	8.301	16.932	36.077	4.381	5.224	8.381
ε_{15}	4	4.922	8.302	16.945	36.083	4.899	5.562	8.412

Table 13: Two-matrix spectrum with loop length truncation $l = 4$.

k	0	0	0	0	0	0.5	0.5	0.5
g_4	0	0.1	1	10	100	0	0.1	1
ε_1	1	1.225	2.024	4.063	8.62	0.707	1.011	1.903
ε_2	1	1.225	2.024	4.07	8.622	1.225	1.421	2.146
ε_3	2	2.314	3.542	6.883	14.46	1.414	1.946	3.444
ε_4	2	2.449	4.05	8.143	17.276	1.932	2.428	4.049
ε_5	2	2.45	4.05	8.148	17.279	2.121	2.777	4.147
ε_6	3	3.54	5.581	10.989	23.189	2.45	2.924	5.285
ε_7	3	3.54	5.581	11.003	23.191	2.639	3.399	5.712
ε_8	3	3.674	6.091	12.197	25.839	2.828	3.818	6.155
ε_9	3	3.674	6.103	12.233	25.913	3.157	3.918	6.215
ε_{10}	4	4.631	7.121	13.881	29.201	3.346	4.163	7.007
ε_{11}	4	4.773	7.684	15.324	32.436	3.535	4.397	7.418
ε_{12}	4	4.774	7.691	15.335	32.469	3.674	4.623	7.609
ε_{13}	4	4.775	7.702	15.386	32.569	3.864	4.84	7.986
ε_{14}	4	4.921	8.301	16.932	36.077	3.864	4.907	8.381
ε_{15}	4	4.922	8.302	16.945	36.083	4.053	5.224	8.412
ε_{16}	5	5.858	9.164	18.058	38.031	4.381	5.378	8.858
ε_{17}	5	5.859	9.175	18.069	38.05	4.571	5.562	9.319
ε_{18}	5	5.998	9.732	19.444	41.179	4.571	5.67	9.48
ε_{19}	5	6.001	9.745	19.47	41.264	4.899	5.831	9.692
ε_{20}	5	6.003	9.808	19.574	41.368	5.088	6.066	9.962
ε_{21}	5	6.008	9.828	19.607	41.464	5.089	6.243	10.222
ε_{22}	5	6.156	10.844	20.795	43.978	5.606	6.614	11.082
ε_{23}	5	6.178	11.257	21.488	44.988	6.124	6.949	11.517

Table 14: Two-matrix spectrum with loop length truncation $l = 5$.

k	0	0	0	0	0	0.5	0.5	0.5
g_4	0	0.1	1	10	100	0	0.1	1
ε_1	1	1.221	2.009	4.029	8.546	0.707	1.009	1.893
ε_2	1	1.222	2.01	4.042	8.552	1.227	1.421	2.137
ε_3	2	2.306	3.535	6.884	14.456	1.413	1.941	3.44
ε_4	2	2.443	4.008	8.061	17.099	1.932	2.423	4.02
ε_5	2	2.45	4.022	8.075	17.108	2.12	2.777	4.127
ε_6	3	3.535	5.576	10.997	23.206	2.453	2.923	5.293
ε_7	3	3.542	5.58	11.013	23.211	2.64	3.395	5.706
ε_8	3	3.682	6.063	12.104	25.62	2.827	3.816	6.138
ε_9	3	3.688	6.077	12.14	25.709	3.159	3.895	6.206
ε_{10}	3.961	4.625	7.081	13.759	28.924	3.347	4.168	6.94
ε_{11}	3.972	4.747	7.583	15.039	31.786	3.536	4.37	7.319
ε_{12}	3.987	4.763	7.59	15.05	31.808	3.68	4.61	7.453
ε_{13}	3.991	4.773	7.609	15.127	31.959	3.863	4.812	7.808
ε_{14}	3.998	4.889	7.923	16.108	34.323	3.865	4.901	8.064
ε_{15}	4	4.907	7.992	16.258	34.534	4.054	5.206	8.156
ε_{16}	4.987	5.863	9.164	18.051	38.027	4.242	5.371	8.857
ε_{17}	4.989	5.866	9.171	18.07	38.045	4.386	5.552	9.312
ε_{18}	4.994	6.002	9.713	19.378	40.997	4.572	5.673	9.475
ε_{19}	4.996	6.01	9.728	19.406	41.036	4.572	5.822	9.669
ε_{20}	4.998	6.019	9.762	19.459	41.193	4.761	5.892	9.919
ε_{21}	4.999	6.032	9.774	19.502	41.28	4.904	6.071	10.206
ε_{22}	4.999	6.158	10.663	20.553	43.419	5.091	6.238	10.508
ε_{23}	5	6.19	10.682	20.776	43.648	5.093	6.357	10.811
ε_{24}	6	6.87	10.988	21.123	44.304	5.272	6.548	10.916
ε_{25}	6	6.955	11.036	22.095	46.691	5.278	6.612	11.115
ε_{26}	6	7.078	11.173	22.176	46.723	5.281	6.688	11.144
ε_{27}	6	7.096	11.205	22.19	46.852	5.611	6.818	11.243
ε_{28}	6.001	7.109	11.219	22.238	46.923	5.796	6.952	11.285
ε_{29}	6.001	7.11	11.244	22.259	46.954	5.799	7.016	11.321
ε_{30}	6.003	7.18	11.391	22.399	47.149	5.8	7.03	11.597
ε_{31}	6.004	7.233	11.735	23.444	49.503	5.811	7.097	11.643
ε_{32}	6.006	7.239	11.834	23.478	49.806	6.129	7.25	11.751
ε_{33}	6.009	7.252	11.921	23.688	49.88	6.315	7.405	11.924
ε_{34}	6.021	7.259	11.972	23.703	50.107	6.316	7.516	12.221
ε_{35}	6.028	7.341	12.001	23.734	50.372	6.324	7.645	12.388
ε_{36}	6.048	7.376	12.961	24.536	51.909	6.836	8.01	13.169
ε_{37}	6.062	7.488	13.176	25.326	53.015	7.352	8.346	13.249

Table 15: Two-matrix spectrum with loop length truncation $l = 6$.

k	0	0	0	0	0	0.5	0.5	0.5
g_4	0	0.1	1	10	100	0	0.1	1
ε_1	1	1.223	2.014	4.022	8.517	0.708	1.012	1.896
ε_2	1	1.225	2.032	4.048	8.643	1.232	1.426	2.139
ε_3	2	2.309	3.559	6.899	14.511	1.411	1.938	3.446
ε_4	2	2.444	4.016	8.011	17.068	1.935	2.428	4.027
ε_5	2	2.452	4.044	8.097	17.156	2.124	2.788	4.11
ε_6	2.904	3.534	5.589	11.001	23.229	2.458	2.925	5.292
ε_7	2.941	3.546	5.627	11.02	23.332	2.642	3.4	5.706
ε_8	2.978	3.679	6.058	12.037	25.643	2.829	3.826	6.11
ε_9	2.982	3.685	6.08	12.141	25.723	3.164	3.898	6.192
ε_{10}	3.904	4.627	7.111	13.798	29.071	3.351	4.186	6.957
ε_{11}	3.93	4.745	7.604	15.055	31.843	3.532	4.378	7.299
ε_{12}	3.959	4.766	7.615	15.076	31.924	3.694	4.611	7.467
ε_{13}	3.974	4.779	7.661	15.112	32.036	3.855	4.819	7.814
ε_{14}	3.986	4.89	7.942	16.077	34.153	3.872	4.867	8.067
ε_{15}	3.991	4.911	8.008	16.222	34.731	4.056	5.223	8.143
ε_{16}	4.79	5.86	9.153	17.907	37.776	4.236	5.348	8.708
ε_{17}	4.889	5.863	9.172	17.929	37.898	4.398	5.563	9.005
ε_{18}	4.911	5.985	9.456	19.035	40.246	4.571	5.67	9.224
ε_{19}	4.931	5.997	9.605	19.125	40.594	4.576	5.801	9.376
ε_{20}	4.963	6.003	9.638	19.148	40.629	4.758	5.889	9.479
ε_{21}	4.975	6.009	9.648	19.209	40.703	4.914	6.07	9.732
ε_{22}	4.985	6.118	9.672	20.067	42.483	4.952	6.222	9.976
ε_{23}	4.996	6.124	9.862	20.21	43.11	5.096	6.357	10.143
ε_{24}	5.978	6.872	10.703	20.807	43.733	5.105	6.549	10.517
ε_{25}	5.982	6.955	11.084	22.147	46.601	5.281	6.608	10.814
ε_{26}	5.99	7.078	11.185	22.211	46.987	5.285	6.703	11.149
ε_{27}	5.991	7.096	11.252	22.223	47.068	5.291	6.822	11.163
ε_{28}	5.993	7.106	11.274	22.262	47.143	5.483	6.863	11.246
ε_{29}	5.994	7.11	11.289	22.33	47.198	5.612	6.883	11.304
ε_{30}	5.997	7.183	11.465	22.604	48.218	5.775	7.013	11.566
ε_{31}	5.999	7.231	11.768	23.39	49.559	5.795	7.11	11.609
ε_{32}	6	7.239	11.828	23.468	49.855	5.806	7.153	11.771
ε_{33}	6.001	7.254	11.922	23.563	50.017	5.815	7.248	11.888
ε_{34}	6.017	7.26	11.952	23.65	50.08	6	7.333	12.222
ε_{35}	6.023	7.325	12.088	23.776	50.145	6.013	7.407	12.36
ε_{36}	6.036	7.366	12.735	24.253	51.73	6.067	7.521	12.383
ε_{37}	6.055	7.478	12.752	24.954	52.707	6.155	7.59	12.811

Table 16: Two-matrix spectrum with loop length truncation $l = 7$.

k	0	0	0	0	0	0.5	0.5	0.5
g_4	0	0.1	1	10	100	0	0.1	1
ε_{38}	7.002	8.135	12.928	25.004	52.799	6.251	7.661	12.835
ε_{39}	7.003	8.138	12.957	25.259	52.943	6.326	7.709	12.971
ε_{40}	7.005	8.227	13.213	26.213	55.46	6.331	7.799	13.026
ε_{41}	7.005	8.239	13.258	26.288	55.632	6.512	7.984	13.136
ε_{42}	7.006	8.31	13.28	26.331	55.74	6.519	8.018	13.196
ε_{43}	7.007	8.317	13.296	26.365	55.848	6.527	8.048	13.267
ε_{44}	7.01	8.328	13.312	26.382	55.965	6.535	8.128	13.372
ε_{45}	7.013	8.337	13.339	26.431	56.117	6.69	8.15	13.463
ε_{46}	7.014	8.345	13.372	26.451	56.198	6.839	8.247	13.479
ε_{47}	7.02	8.352	13.451	26.562	56.373	7.029	8.273	13.532
ε_{48}	7.022	8.362	13.505	26.589	56.564	7.035	8.441	13.575
ε_{49}	7.027	8.364	13.794	27.287	58.281	7.044	8.472	13.815
ε_{50}	7.038	8.451	13.98	27.505	58.424	7.048	8.54	13.86
ε_{51}	7.06	8.463	14.006	27.596	58.785	7.066	8.637	13.925
ε_{52}	7.076	8.483	14.044	27.833	59.008	7.374	8.681	14.114
ε_{53}	7.1	8.493	14.158	27.944	59.054	7.555	8.834	14.215
ε_{54}	7.163	8.56	14.33	28.048	59.322	7.567	8.992	14.488
ε_{55}	7.263	8.59	14.386	28.09	60.142	7.572	9.076	14.581
ε_{56}	7.345	8.643	15.172	28.787	60.705	8.081	9.408	15.485
ε_{57}	7.499	8.648	15.648	29.561	61.502	8.588	9.756	16.25

Table 17: Two-matrix spectrum with loop length truncation $l = 7$ continued.

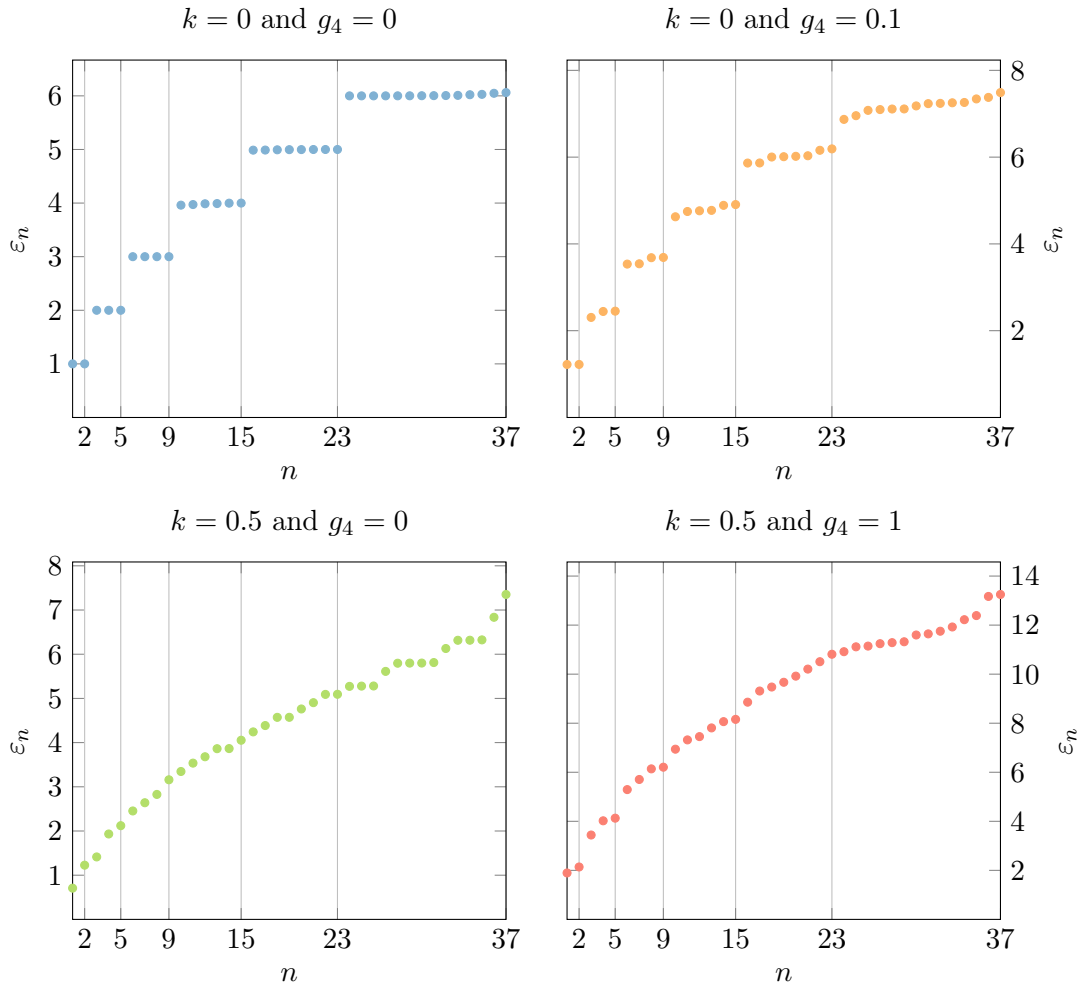


Figure 3: Two-matrix spectrum plots and degeneracy lifting due to g_4 and k .

6 Conclusions

We have applied previously developed numerical, master field methods to solve a variety of coupled two-matrix models. These include matrix integrals and matrix quantum mechanics systems, with the fact that they all have a representation in terms of collective Hamiltonians with (Wilson) loops as dynamical variables. The collective loop space representation provides (nonlinear) Wilson loop equations, which in the former case (matrix integral) are equivalent to Schwinger-Dyson (Migdal-Makeenko) equations. Solution as it was understood in the original minimization schemes is to be accomplished subject to loop space (Schwarz) inequalities which define the constrained minimization procedure. The collective method includes not only the form of the large N Hamiltonian and potential but also provides a complete set of inequalities, which we give in explicit determinate form). The associated (constrained) minimization of the large N problem is implemented through a master field, as explained in detail in the text (and also in original works). The numerical solution of the nonlinear large N stationary point not only gives the leading large N Wilson loop background, it also establishes in concrete terms the existence of the master field. This existence. was questioned through the years in various works. Constrained minimization, which is accomplished with fairly large number of (loop) variables ($\sim 10^4$) is seen to give essentially exact results for large N expectation values, ground state energy and low lying spectra. This size can be further increased for added precision. The formulation, and methods developed are such that there is no difference in having larger number of matrix variables. The large N dynamics is evaluated in loop space, which is parametrized the same way (and easily computer augmented). Regarding further works, and applications of the methods developed in this work, one can contemplate many physical problems requiring understanding through matrix models range from confinement [53] to cosmology [54]. More specifically, extensions to supersymmetric versions of the multi-matrix QM can be considered. The four matrix BMN quantum mechanics (at large N) is clearly accessible by this scheme, and we plan to present results in future work. Considering the two matrix case, whose solution is accomplished in this work, an interesting application to entanglement [55], thermodynamics and the matrix thermofield double (TFD) states. In general this requires a study of QM defined on the Schwinger-Keldysh contour [56, 57]. The TFD state and the corresponding wave functional of the $O(N)$ vector theory based on the collective field formulation was recently studied in [58]. Adjusting our optimization to matrix systems appears possible. An approximate version of the TFD involves coupling the system through single trace interaction [59–61], this corresponds to interaction term in QM that we studied, therefore these models provide a possibility to simulate temperature in the ground state. Likewise will be a fuller exploration of the phase structure of this theory.

Acknowledgments

The work of RdMK, AJ and JPR is partially funded by a Simons Foundation Grant, Award ID 509116. The work of RdMK is also supported by the South African Research

Chairs initiative of the Department of Science and Technology and the National Research Foundation.

A Analytic Results for Matrix Integrals

For the cases with $k = 0$ we can use the techniques [62] to get values of loops that the numerics must reproduce. When $k \neq 0$ but $g_3 = g_4 = 0$ we are left with a quadratic integral which is easily performed.

A.1 Quartic Model

For the matrix integral with action

$$S = \frac{1}{2} \text{Tr} M^2 + \frac{g_4}{N} \text{Tr} M^4. \quad (\text{A.1})$$

The density of eigenvalues obeys

$$\int_{-2a}^{2a} \frac{\phi(y)}{x-y} dy = \frac{1}{x} + 2g_4 x^3, \quad |x| \leq 2a, \quad (\text{A.2})$$

and the normalization condition

$$\int_{-2a}^{2a} \phi(x) dx = 1. \quad (\text{A.3})$$

This is solved by

$$\phi(x) = \frac{1}{\pi} \left(\frac{1}{2} + 4g_4 a^2 + 2g_4 x^2 \right) \sqrt{4a^2 - x^2}, \quad (\text{A.4})$$

where

$$12g_4 a^4 + a^2 - 1 = 0. \quad (\text{A.5})$$

Using this density we compute the following planar expectation values

$$\frac{1}{N^2} \langle \text{Tr} M^2 \rangle = \int_{-2a}^{2a} \phi(x) x^2 dx = \frac{\sqrt{48g_4 + 1} + 24g_4 (2\sqrt{48g_4 + 1} - 3) - 1}{864g_4^2} \quad (\text{A.6})$$

$$\frac{1}{N^3} \langle \text{Tr} M^4 \rangle = \int_{-2a}^{2a} \phi(x) x^4 dx = \frac{-\sqrt{48g_4 + 1} + 24g_4 (36g_4 - 2\sqrt{48g_4 + 1} + 3) + 1}{3456g_4^3} \quad (\text{A.7})$$

$$\begin{aligned} \frac{1}{N^4} \langle \text{Tr} M^6 \rangle &= \int_{-2a}^{2a} \phi(x) x^6 dx \\ &= \frac{\sqrt{48g_4 + 1} + 8g_4 (7\sqrt{48g_4 + 1} + 12g_4 (4\sqrt{48g_4 + 1} - 15) - 10) - 1}{13824g_4^4} \end{aligned} \quad (\text{A.8})$$

$$\begin{aligned}
\frac{1}{N^5} \langle \text{Tr} M^8 \rangle &= \int_{-2a}^{2a} \phi(x) x^8 dx \\
&= -\frac{7}{373248g_4^5} \left[\sqrt{48g_4 + 1} - 1 \right. \\
&\quad \left. - 6g_4 \left(-11\sqrt{48g_4 + 1} + 72g_4 \left(20g_4 - 2\sqrt{48g_4 + 1} + 5 \right) + 15 \right) \right]. \quad (\text{A.9})
\end{aligned}$$

A.2 Quadratic Two-Matrix Model

Doing the Gaussian integrals its simple to find

$$\begin{aligned}
\frac{1}{N^2} \langle \text{Tr}(M_1^2) \rangle &= \frac{1}{1-k^2} & \frac{1}{N^2} \langle \text{Tr}(M_1 M_2) \rangle &= -\frac{k}{1-k^2} \\
\frac{1}{N^3} \langle \text{Tr} M_1^4 \rangle &= \frac{2}{(1-k^2)^2} & \frac{1}{N^3} \langle \text{Tr}(M_1^2 M_2^2) \rangle &= \frac{1+k^2}{1-k^2} \\
\frac{1}{N^4} \langle \text{Tr}(M_1^6) \rangle &= \frac{5}{(1-k^2)^3} & \frac{1}{N^4} \langle \text{Tr} M_1^2 M_2^4 \rangle &= \frac{2+3k^2}{(1-k^2)^3} \\
\frac{1}{N^4} \langle \text{Tr}(M_1^4 M_2^2) \rangle &= \frac{2+3k^2}{(1-k^2)^3} & \frac{1}{N^5} \langle \text{Tr}(M_1^4 M_2^4) \rangle &= \frac{4+9k^2+k^4}{(1-k^2)^4} \\
\frac{1}{N^6} \langle \text{Tr}(M_1^{10}) \rangle &= \frac{42}{(1-k^2)^5} & \frac{1}{N^6} \langle \text{Tr}(M_1^4 M_2^4) \rangle &= \frac{14+28k^2}{(1-k^2)^5} \\
\frac{1}{N^6} \langle \text{Tr}(M_1^5 M_2^5) \rangle &= \frac{25k+16k^3+k^5}{(1-k^2)^5} & \frac{1}{N^7} \langle \text{Tr}(M_1^{12}) \rangle &= \frac{132}{(1-k^2)^6} \\
\frac{1}{N^7} \langle \text{Tr}(M_1^6 M_2^6) \rangle &= \frac{25+81k^2+25k^4+k^6}{(1-k^2)^6} & \frac{1}{N^8} \langle \text{Tr}(M_1^{14}) \rangle &= \frac{429}{(1-k^2)^7} \\
\frac{1}{N^8} \langle \text{Tr}(M_1^{10} M_2^4) \rangle &= \frac{3(25k^4+90k^2+28)}{(1-k^2)^7} & \frac{1}{N^9} \langle \text{Tr}(M_1^{16}) \rangle &= \frac{1430}{(1-k^2)^8} \quad (\text{A.10})
\end{aligned}$$

A.3 Cubic Model

For the matrix integral with action

$$S = \frac{1}{2} \text{Tr} M^2 + \frac{g_3}{\sqrt{N}} \text{Tr} M^3. \quad (\text{A.11})$$

The density of eigenvalues obeys

$$\int_{2a}^{2b} \frac{\phi(y)}{x-y} dy = \frac{1}{x} + \frac{3}{2} g_3 x^3, \quad 2a \leq x \leq 2b, \quad (\text{A.12})$$

and the normalization condition

$$\int_{2a}^{2b} \phi(x) dx = 1. \quad (\text{A.13})$$

This is solved by

$$\phi(x) = \frac{1}{\pi} (1 + 3g_3(a+b) + 3g_3x) \sqrt{(x-2a)(2b-x)}, \quad (\text{A.14})$$

with a and b obtained from

$$3g_3(b-a)^2 + 2(a+b)[1 + 3g_3(a+b)] = 0, \quad (\text{A.15})$$

$$(b-a)^2[1 + 6g_3(a+b)] = 4. \quad (\text{A.16})$$

The solutions to these equations are ugly, so we will plug in definite values of g_3 . Note that we must take $g_3^2 < \frac{1}{108\sqrt{3}} \approx 0.00534$ to get convergence of planar perturbation theory. We take $g_3 = 0.01$ ($a = -1.03198$ and $b = 0.971651$), $g_3 = 0.025$ ($a = -1.08956$ and $b = 0.934167$), and $g_3 = 0.05$ ($a = -1.23513$ and $b = 0.880559$). Using this density we compute the following planar expectation values

$$\begin{aligned} \frac{1}{N^{3/2}} \langle \text{Tr} M \rangle &= \int_{2a}^{2b} \phi(x)x \, dx = -0.0301088 \quad (g = 0.01), \\ &= -0.0767683 \quad (g = 0.025), \\ &= -0.166732 \quad (g = 0.05). \end{aligned} \quad (\text{A.17})$$

$$\begin{aligned} \frac{1}{N^2} \langle \text{Tr} M^2 \rangle &= \int_{2a}^{2b} \phi(x)x^2 \, dx = 1.00363 \quad (g = 0.01), \\ &= 1.02358 \quad (g = 0.025), \\ &= 1.11155 \quad (g = 0.05). \end{aligned} \quad (\text{A.18})$$

$$\begin{aligned} \frac{1}{N^3} \langle \text{Tr} M^4 \rangle &= \int_{2a}^{2b} \phi(x)x^4 \, dx = 2.02182 \quad (g = 0.01), \\ &= 2.14427 \quad (g = 0.025), \\ &= 2.73465 \quad (g = 0.05). \end{aligned} \quad (\text{A.19})$$

$$\begin{aligned} \frac{1}{N^4} \langle \text{Tr} M^6 \rangle &= \int_{2a}^{2b} \phi(x)x^6 \, dx = 5.10951 \quad (g = 0.01), \\ &= 5.73859 \quad (g = 0.025), \\ &= 9.1135 \quad (g = 0.05). \end{aligned} \quad (\text{A.20})$$

B Analytical Results of The One-Matrix Quantum Mechanics

We consider the hermitian one-matrix quantum mechanics with a quartic interaction

$$H = -\frac{1}{2} \text{Tr} \left(\frac{\partial^2}{\partial M^2} \right) + \frac{1}{2} \text{Tr}(M^2) + \frac{g_4}{N} \text{Tr}(M^4). \quad (\text{B.1})$$

This model is dual to the $D = 1$ string theory in the double scaling limit. The model was first solved in [19] and its spectrum was solved in [11] using a field theoretic approach. We briefly summarize the analytical results derived there.

Eigenvalue distribution. In the large N limit the eigenvalue distribution of the ground state [36, 62] is

$$\phi_0(x) = \frac{1}{\pi} \sqrt{\Lambda^2 + 2g_4\Lambda^4 - x^2 - 2g_4x^4}, \quad (\text{B.2})$$

where $x \in [-\Lambda, \Lambda]$, and Λ is determined by the constraint

$$\int_{-\Lambda}^{\Lambda} \phi_0(x) dx = \frac{\Lambda^2}{2} \sqrt{1 + 2g_4\Lambda^2} {}_2F_1\left(-\frac{1}{2}, \frac{1}{2}, 2; -\frac{2g_4\Lambda^2}{1 + 2g_4\Lambda^2}\right) = 1. \quad (\text{B.3})$$

The constraint is saturated at the critical value $g_c = -1/3\sqrt{2}\pi$.

Loop values. The loops at the ground state are

$$\begin{aligned} \phi(2C) &\equiv \frac{\text{Tr}(M^{2C})}{N^{C+1}} = \int_{-\Lambda}^{\Lambda} \phi_0(x) x^{2C} dx \\ &= \frac{\Lambda^{2C+2} \sqrt{1 + 2g_4\Lambda^2} \Gamma(C + \frac{1}{2})}{2\sqrt{\pi} \Gamma(C + 2)} {}_2F_1\left(-\frac{1}{2}, C + \frac{1}{2}, C + 2; -\frac{2g_4\Lambda^2}{1 + 2g_4\Lambda^2}\right), \end{aligned} \quad (\text{B.4})$$

and all loops with odd powers are zero.

Ground state energy. The leading ground state energy is

$$E_{\text{gs}}^{(0)} = \frac{1}{2}\Lambda^2 (1 + 2g\Lambda^2) - \frac{1}{8}\Lambda^4 (1 + 2g_4\Lambda^2)^{3/2} {}_2F_1\left(-\frac{3}{2}, \frac{1}{2}, 3; -\frac{2g_4\Lambda^2}{1 + 2g_4\Lambda^2}\right). \quad (\text{B.5})$$

In the free case we have $E_{\text{gs}}^{(0)} = 1/2$. Figure 4 shows the results obtained from the above analytic expression, as well as the collective potential $V_{\text{eff}}^{(0)}$ values, demonstrating an excellent agreement.

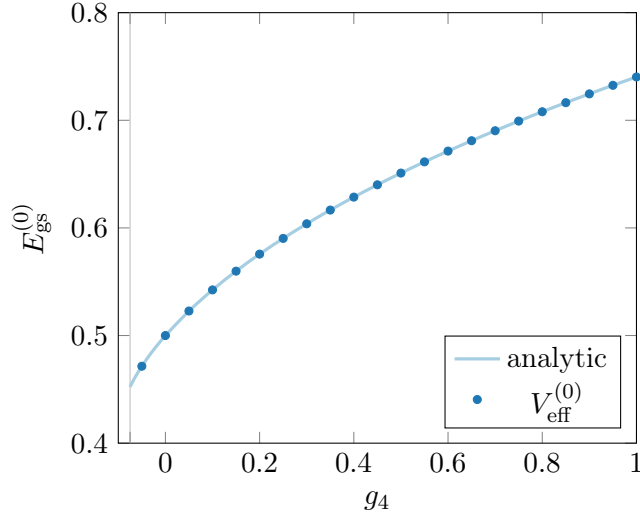


Figure 4: One-matrix $E_{\text{gs}}^{(0)}$ versus the quartic coupling g_4 .

Spectrum. In the large N limit the spectrum of small fluctuations is

$$\varepsilon_n(g_4) = \frac{n\pi}{2} \left[\int_0^\Lambda \frac{dx}{\pi\phi_0(x)} \right]^{-1}. \quad (\text{B.6})$$

The integral can be evaluated analytically

$$\varepsilon_n(g_4) = \frac{n\pi}{2} \sqrt{1 + 2g_4\Lambda^2} \left[K \left(\sqrt{\frac{-2g_4\Lambda^2}{1 + 2g_4\Lambda^2}} \right) \right]^{-1}, \quad (\text{B.7})$$

where K is the complete elliptic integral of the first kind. The general feature of (B.7) is that the level n frequency is proportional to n , no matter how g_4 varies. One thus expects that the spectrum fits a straight line when plotted as a function of level number.

References

- [1] J. Hoppe, *QUANTUM THEORY OF A RELATIVISTIC SURFACE*, in *Workshop on Constraint's Theory and Relativistic Dynamics*, pp. 267–276, 1986.
- [2] V.A. Kazakov, *Solvable matrix models*, [hep-th/0003064](#).
- [3] S. Corley, A. Jevicki and S. Ramgoolam, *Exact correlators of giant gravitons from dual $N=4$ SYM theory*, *Adv. Theor. Math. Phys.* **5** (2002) 809 [[hep-th/0111222](#)].
- [4] P. Haggi-Mani and B. Sundborg, *Free large N supersymmetric Yang-Mills theory as a string theory*, *JHEP* **04** (2000) 031 [[hep-th/0002189](#)].
- [5] O. Aharony, J. Marsano, S. Minwalla, K. Papadodimas and M. Van Raamsdonk, *The Hagedorn - deconfinement phase transition in weakly coupled large N gauge theories*, *Adv. Theor. Math. Phys.* **8** (2004) 603 [[hep-th/0310285](#)].
- [6] N. Ishibashi, H. Kawai, Y. Kitazawa and A. Tsuchiya, *A Large N reduced model as superstring*, *Nucl. Phys. B* **498** (1997) 467 [[hep-th/9612115](#)].
- [7] D.E. Berenstein, J.M. Maldacena and H.S. Nastase, *Strings in flat space and pp waves from $N=4$ superYang-Mills*, *JHEP* **04** (2002) 013 [[hep-th/0202021](#)].
- [8] R. de Mello Koch, A. Jevicki and J.P. Rodrigues, *Collective string field theory of matrix models in the BMN limit*, *Int. J. Mod. Phys. A* **19** (2004) 1747 [[hep-th/0209155](#)].
- [9] B. Balthazar, V.A. Rodriguez and X. Yin, *The $c = 1$ string theory S-matrix revisited*, *JHEP* **04** (2019) 145 [[1705.07151](#)].
- [10] A. Sen, *D-instantons, string field theory and two dimensional string theory*, *JHEP* **11** (2021) 061 [[2012.11624](#)].
- [11] S.R. Das and A. Jevicki, *String Field Theory and Physical Interpretation of $D = 1$ Strings*, *Mod. Phys. Lett. A* **5** (1990) 1639.
- [12] N. Ishibashi and H. Kawai, *String field theory of $c \leq 1$ noncritical strings*, *Phys. Lett. B* **322** (1994) 67 [[hep-th/9312047](#)].
- [13] A. Jevicki and J.P. Rodrigues, *Loop space Hamiltonians and field theory of noncritical strings*, *Nucl. Phys. B* **421** (1994) 278 [[hep-th/9312118](#)].
- [14] M. Mariño, *Lectures on non-perturbative effects in large N gauge theories, matrix models and strings*, *Fortsch. Phys.* **62** (2014) 455 [[1206.6272](#)].

- [15] H. Gharibyan, M. Hanada, M. Honda and J. Liu, *Toward simulating Superstring/M-theory on a quantum computer*, *JHEP* **07** (2021) 140 [[2011.06573](#)].
- [16] F. David, *Planar Diagrams, Two-Dimensional Lattice Gravity and Surface Models*, *Nucl. Phys. B* **257** (1985) 45.
- [17] V.A. Kazakov, *Bilocal Regularization of Models of Random Surfaces*, *Phys. Lett. B* **150** (1985) 282.
- [18] V.A. Kazakov, A.A. Migdal and I.K. Kostov, *Critical Properties of Randomly Triangulated Planar Random Surfaces*, *Phys. Lett. B* **157** (1985) 295.
- [19] V.A. Kazakov and A.A. Migdal, *Recent Progress in the Theory of Noncritical Strings*, *Nucl. Phys. B* **311** (1988) 171.
- [20] D.J. Gross and N. Miljkovic, *A Nonperturbative Solution of $D = 1$ String Theory*, *Phys. Lett. B* **238** (1990) 217.
- [21] E. Brezin, V.A. Kazakov and A.B. Zamolodchikov, *Scaling Violation in a Field Theory of Closed Strings in One Physical Dimension*, *Nucl. Phys. B* **338** (1990) 673.
- [22] P.H. Ginsparg and J. Zinn-Justin, *2-d GRAVITY + 1-d MATTER*, *Phys. Lett. B* **240** (1990) 333.
- [23] D.J. Gross and I.R. Klebanov, *Vortices and the nonsinglet sector of the $c = 1$ matrix model*, *Nucl. Phys. B* **354** (1991) 459.
- [24] S. Dalley and I.R. Klebanov, *String spectrum of $(1+1)$ -dimensional large N QCD with adjoint matter*, *Phys. Rev. D* **47** (1993) 2517 [[hep-th/9209049](#)].
- [25] V. Kazakov, I.K. Kostov and D. Kutasov, *A Matrix model for the two-dimensional black hole*, *Nucl. Phys. B* **622** (2002) 141 [[hep-th/0101011](#)].
- [26] J.M. Maldacena, *Long strings in two dimensional string theory and non-singlets in the matrix model*, *JHEP* **09** (2005) 078 [[hep-th/0503112](#)].
- [27] B. Balthazar, V.A. Rodriguez and X. Yin, *Long String Scattering in $c = 1$ String Theory*, *JHEP* **01** (2019) 173 [[1810.07233](#)].
- [28] P. Betzios and O. Papadoulaki, *FZZT branes and non-singlets of matrix quantum mechanics*, *JHEP* **07** (2020) 157 [[1711.04369](#)].
- [29] D.A. Lowe and L. Thorlacius, *Black hole holography and mean field evolution*, *JHEP* **01** (2018) 049 [[1710.03302](#)].
- [30] I. Amado, B. Sundborg, L. Thorlacius and N. Wintergerst, *Black holes from large N singlet models*, *JHEP* **03** (2018) 075 [[1712.06963](#)].
- [31] J.S. Cotler, G. Gur-Ari, M. Hanada, J. Polchinski, P. Saad, S.H. Shenker et al., *Black Holes and Random Matrices*, *JHEP* **05** (2017) 118 [[1611.04650](#)].
- [32] K.N. Anagnostopoulos, M. Hanada, J. Nishimura and S. Takeuchi, *Monte Carlo studies of supersymmetric matrix quantum mechanics with sixteen supercharges at finite temperature*, *Phys. Rev. Lett.* **100** (2008) 021601 [[0707.4454](#)].
- [33] B. Lucini, M. Teper and U. Wenger, *The High temperature phase transition in $SU(N)$ gauge theories*, *JHEP* **01** (2004) 061 [[hep-lat/0307017](#)].
- [34] Y.M. Makeenko and A.A. Migdal, *Exact Equation for the Loop Average in Multicolor QCD*, *Phys. Lett. B* **88** (1979) 135.

- [35] A. Jevicki and B. Sakita, *Collective Field Approach to the Large N Limit: Euclidean Field Theories*, *Nucl. Phys. B* **185** (1981) 89.
- [36] A. Jevicki and B. Sakita, *The Quantum Collective Field Method and Its Application to the Planar Limit*, *Nucl. Phys. B* **165** (1980) 511.
- [37] A. Jevicki, O. Karim, J.P. Rodrigues and H. Levine, *Loop Space Hamiltonians and Numerical Methods for Large N Gauge Theories*, *Nucl. Phys. B* **213** (1983) 169.
- [38] A. Jevicki, O. Karim, J.P. Rodrigues and H. Levine, *Loop Space Hamiltonians and Numerical Methods for Large N Gauge Theories. 2.*, *Nucl. Phys. B* **230** (1984) 299.
- [39] J.P. Rodrigues, *Loop Space, Master Variables and The Spectrum in The Large N Limit*, Ph.D. thesis, Brown University, 1983.
- [40] A. Jevicki and J.P. Rodrigues, *Master Variables and Spectrum Equations in Large N Theories*, *Nucl. Phys. B* **230** (1984) 317.
- [41] P.D. Anderson and M. Kruczenski, *Loop Equations and bootstrap methods in the lattice*, *Nucl. Phys. B* **921** (2017) 702 [[1612.08140](#)].
- [42] H.W. Lin, *Bootstraps to strings: solving random matrix models with positvite*, *JHEP* **06** (2020) 090 [[2002.08387](#)].
- [43] X. Han, S.A. Hartnoll and J. Kruthoff, *Bootstrapping Matrix Quantum Mechanics*, *Phys. Rev. Lett.* **125** (2020) 041601 [[2004.10212](#)].
- [44] V. Kazakov and Z. Zheng, *Analytic and Numerical Bootstrap for One-Matrix Model and "Unsolvable" Two-Matrix Model*, **2108.04830**.
- [45] J.P. Rodrigues, *Numerical Solution of Lattice Schwinger-dyson Equations in the Large N Limit*, *Nucl. Phys. B* **260** (1985) 350.
- [46] E. Marinari and G. Parisi, *The Supersymmetric One-dimensional String*, *Phys. Lett. B* **240** (1990) 375.
- [47] D.J. Gross and E. Witten, *Possible Third Order Phase Transition in the Large N Lattice Gauge Theory*, *Phys. Rev. D* **21** (1980) 446.
- [48] A. Jevicki and B. Sakita, *Loop Space Representation and the Large N Behavior of the One Plaquette Kogut-Susskind Hamiltonian*, *Phys. Rev. D* **22** (1980) 467.
- [49] J.P. Rodrigues, *Variant Actions and the Presence of a Gross-witten Phase Transition*, *Phys. Rev. D* **26** (1982) 2833.
- [50] J.P. Rodrigues, *EXACT PHASE STRUCTURE OF LARGE N ONE PLAQUETTE HAMILTONIAN LATTICE QCD WITH MIXED FUNDAMENTAL ADJOINT POTENTIAL*, *Phys. Rev. D* **26** (1982) 2940.
- [51] V.A. Kostelecky and S. Samuel, *The Static Tachyon Potential in the Open Bosonic String Theory*, *Phys. Lett. B* **207** (1988) 169.
- [52] M. Bianchi, J.F. Morales and H. Samtleben, *On stringy AdS(5) x S**5 and higher spin holography*, *JHEP* **07** (2003) 062 [[hep-th/0305052](#)].
- [53] M. Hanada, A. Jevicki, C. Peng and N. Wintergerst, *Anatomy of Deconfinement*, *JHEP* **12** (2019) 167 [[1909.09118](#)].
- [54] S. Brahma, R. Brandenberger and S. Laliberte, *Emergent Cosmology from Matrix Theory*, **2107.11512**.

- [55] S.R. Das, A. Kaushal, G. Mandal and S.P. Trivedi, *Bulk Entanglement Entropy and Matrices*, *J. Phys. A* **53** (2020) 444002 [[2004.00613](#)].
- [56] J.S. Schwinger, *Brownian motion of a quantum oscillator*, *J. Math. Phys.* **2** (1961) 407.
- [57] L.V. Keldysh, *Diagram technique for nonequilibrium processes*, *Zh. Eksp. Teor. Fiz.* **47** (1964) 1515.
- [58] A. Jevicki, X. Liu, J. Yoon and J. Zheng, *Dynamical Symmetry and the Thermofield State at Large N* , [2109.13381](#).
- [59] J. Maldacena and X.-L. Qi, *Eternal traversable wormhole*, [1804.00491](#).
- [60] F. Alet, M. Hanada, A. Jevicki and C. Peng, *Entanglement and Confinement in Coupled Quantum Systems*, *JHEP* **02** (2021) 034 [[2001.03158](#)].
- [61] S. Plugge, E. Lantagne-Hurtubise and M. Franz, *Revival Dynamics in a Traversable Wormhole*, *Phys. Rev. Lett.* **124** (2020) 221601 [[2003.03914](#)].
- [62] E. Brezin, C. Itzykson, G. Parisi and J.B. Zuber, *Planar Diagrams*, *Commun. Math. Phys.* **59** (1978) 35.